Periodico di Mineralogia (2015), 84, 3B (Special Issue), 657-699 DOI: 10.2451/2015PM0455

PERIODICO di MINERALOGIA
established in 1930

An International Journal of
MINERALOGY, CRYSTALLOGRAPHY, GEOCHEMISTRY,
ORE DEPOSITS, PETROLOGY, VOLCANOLOGY
and applied topics on Environment, Archaeometry and Cultural Heritage

Continental collision from two perspectives: a review of Variscan metamorphism and deformation in northern Sardinia

Gabriele Cruciani[1,*], Chiara Montomoli[2], Rodolfo Carosi[3], Marcello Franceschelli[1] and Mariano Puxeddu[4]

[1] Dipartimento di Scienze Chimiche e Geologiche, Via Trentino, 51, 09127 Cagliari, Italy
[2] Dipartimento di Scienze della Terra, V. S. Maria, 53, 56126 Pisa, Italy
[3] Dipartimento di Scienze della Terra, V. V. Caluso, 35, 10125 Torino, Italy
[4] Former researcher of the Istituto di Geoscienze e Georisorse CNR-Pisa, Via Moruzzi, 1, 56124 Pisa, Italy
* Corresponding Author: *gcrucian@unica.it*

Abstract

Structural, petrological and geochronological data from the Variscan chain of northern Sardinia are discussed, with the aim to improve our knowledge on the tectono-metamorphic evolution of the northern Sardinian basement and its role in the tectonic puzzle of the southern Variscan massifs. In northern Sardinia, which corresponds to the Inner zone of the chain, the metamorphic grade rapidly increases towards the NE from biotite to sillimanite+K-feldspar zone. The highest grade rocks cropping out in the Migmatite zone reached amphibolite facies conditions in the sedimentary and igneous-derived migmatite and eclogite/granulite facies in the enclosed metabasite lenses. Evidence of HP metamorphism has also recently been found more to the south in micaschist from the garnet zone. The D_1 deformation can be observed in the southern part of the Inner zone, whereas, moving progressively northwards, the D_2 deformation progressively obliterates the previous foliation. The other, less pervasive, deformation phases (D_3, D_4, D_5) are sometimes recognizable in the outcrop localities, but they are not as ubiquitous as the previous D_1 and D_2. HP metamorphism in metabasites and schists is related to the collision and/or northwards-directed subduction of the continental crust, which was part of the northern Gondwana or peri-Gondwanian terranes in Early Palaeozoic times. The HP metamorphism, which is pre- to syn-D_1, was followed by Barrovian metamorphism. The stacking of metamorphic sequences with the building up of the nappe pile was a consequence of the High Grade Metamorphic Complex exhumation. This was activated by NW-SE striking and top-to-the S and SW shear zones and faults with a major dip-slip component of movement, coeval with the late phase of the D_1 deformation. Transpressional deformation then developed until the High-Grade Metamorphic Complex continued to be exhumed and the Low- to Medium-Grade Metamorphic Complex was

underthrust to the north. Finally, the extensional tectonic regime was accompanied by local occurrences of HT-LP metamorphism. Deformation and metamorphism in the Sardinian Variscides were accompanied by the intrusion of igneous suites of the Sardinia-Corsica batholith, which was emplaced during the Middle Carboniferous/Permian post-collisional phase.

Key words: Sardinian chain; deformation history; metamorphic evolution; P-T-t path; tectonic setting; Variscan orogeny.

Introduction

The Variscan basement in Sardinia offers good and continuous exposures of metamorphic rocks. This allows the progressive metamorphism and deformation across sections of an orogenic system that are now exhumed to the surface to be tracked. Moreover, the observation of large portions of exhumed deep crustal levels enables the structures and kinematics connected to deep crustal processes to be directly observed.

This led several authors to get involved in the study of the northern Sardinia basement as early as the 1970s. After some work carried out in specific key areas (Miller et al., 1976; Carmignani et al., 1979; Ghezzo et al., 1979), the general features of the metamorphism were outlined by Franceschelli et al. (1982a), who discovered a prograde Barrovian-type metamorphic zonation from SW to NE Sardinia. In the early 1990s, the Sardinian transect of the Variscan chain was already depicted as a complex tectono-metamorphic basement made up, from SW to NE, of a Foreland zone (Sulcis Iglesiente), a Nappe zone (central Sardinia), and an Inner zone (northern Sardinia) (Carmignani et al., 1992; 1994). In this period, Cappelli et al. (1992) suggested the occurrence of a Variscan suture in northern Sardinia based on the finding of eclogitic relics in metabasites with MORB affinity entrapped within the mylonitic belt that runs from Posada (NE) to Asinara Island (NW Sardinia).

It was in the new millennium that the several new structural, geopetrographical and geochemical studies carried out in the metamorphic Variscan basement of NE Sardinia by the research groups of Cagliari, Pisa, Torino, Genova and Sassari universities contributed significantly to both identify the late D_1 shear zones related to the start of exhumation and clarify the relationships between the D_2 phase and the basement exhumation. Important contributions were also provided by the $^{40}Ar/^{39}Ar$ dating of the D_1 and D_2 deformation phases (Di Vincenzo et al., 2004), and by the zircon and monazite U-Pb dating of the D_2 transpressional phase (Carosi et al., 2012).

Finally, the recognition of sinistral shear zones along the Posada-Asinara line, the discovery of the staurolite + biotite pair many kilometres south of the previously defined staurolite + biotite isograd (Carosi et al., 2008), and the recognition of HP metamorphism during the D_1 phase in chloritoid schists from the Low- to Medium-Grade Metamorphic Complex (Cruciani et al., 2013a) improved the knowledge on the deformational, kinematic and thermobaric history of this important transect of the Variscan chain.

However, the following aspects are still unresolved, and require further study in the near future: (i) the occurrence and position of an eventual oceanic suture; (ii) the pre-Variscan evolution of the Sardinian basement; (iii) the areal extension of the HP, D_1 event; and (iv) the position of the Corsica-Sardinia microplate in the Upper Palaeozoic south Variscan puzzle. The aim of this paper is to provide an exhaustive review on the current knowledge on the Variscan basement of NE Sardinia.

The Sardinian Variscan Belt

The present position of the Corsica-Sardinia microplate in the western Mediterranean Sea is the result of a 30° anticlockwise southwards rotation of a fragment of the southern European margin. The rifting process that separated the Corsica-Sardinia block from Provence is referred to the Oligocene (30-24 Ma, Séranne, 1999; Gattacecca, 2001). A following oceanic accretion took place during the Miocene between 23 and 15 Ma (Ferrandini et al., 2000; 2003 and related bibliography). An opposite fictitious clockwise rotation of the Corsica-Sardinia microplate is therefore necessary to ascertain the original Variscan structural directions. Most of the Corsica-Sardinia Palaeozoic basement was intruded by a huge batholith in the 340-280 Ma time range.

The basement consists of metaigneous to metasedimentary sequences ranging in age from the Cambrian to the Lower Carboniferous and from the Late Carboniferous to Permian igneous rocks.

Carboniferous-Permian sedimentary basins (Barca et al., 1995) and Permian volcanism cover the crystalline basement rocks.

In the Sardinian branch of the Variscan Belt (Figure 1), three main structural zones can be distinguished from SW to NE (Carmignani et al.,1982a; 1994; 2001): (i) in SW Sardinia (Sulcis-Iglesiente), a Foreland zone is made up of metasedimentary sequences that are Upper Vendian to Lower Carboniferous in age and characterized by very low- to low-grade metamorphism; (ii) a SW-vergent nappe stacking, known as the Nappe zone, whose low-grade metamorphic rocks form a Palaeozoic metasedimentary succession that includes thick calc-alkali volcanic sequences that are Middle Ordovician in age (Carmignani et al., 1994; Oggiano et al. 2010; Cruciani et al., 2013b). The Nappe zone is further subdivided into an external and internal Nappe zone; and (iii) an Inner zone made up of medium- to high-grade metamorphic rocks intruded by Upper Palaeozoic igneous rocks.

Two main metamorphic complexes (Figure 1) can be distinguished in this Inner zone (Carmignani et al., 1994; 2001):

a) A polyphase High-Grade Metamorphic Complex (HGMC) consisting of diatexites and metatexites, including sporadic amphibolite bodies that were lately re-equilibrated in HT-LP conditions. The entire HGMC outcrops in north Sardinia and southern Corsica, but still preserves relict eclogite/granulite assemblages of high to intermediate pressures of an unknown age (Miller et al., 1976; Ghezzo et al., 1979; Franceschelli et al., 1982a; Di Pisa et al., 1993).

b) A Low- to Medium-Grade Metamorphic Complex (L-MGMC) mainly made up of metapelitic micaschists and paragneisses (Franceschelli et al., 1982a), with locally embedded quartzite and metabasite bodies (Cappelli et al., 1992; Cruciani et al., 2010, 2011a).

A large Variscan transpressive shear belt (Carosi and Palmeri, 2002; Iacopini et al., 2008; Carosi et al., 2009), which was previously interpreted as a late Variscan strike-slip shear zone (Elter et al., 1990), developed at the boundary between the HGMC and L-MGMC, and is easily recognizable in outcrops along the Posada Valley, in southern Gallura, and within Asinara Island (Figure 1) (Oggiano and Di Pisa, 1992; Carmignani and Oggiano, 1997; Carosi et al., 2004a; 2005; 2009). Locally, where Variscan dextral transpression has not obliterated the previous tectonic structures (Oggiano and Di Pisa, 1992; Carosi and Palmeri, 2002; Carosi et al., 2004a; 2005; 2008; 2009; 2012; Frassi et al., 2009), it is possible to discern the thrusting of the HGMC onto the L-MGMC.

General overview of Variscan deformation in northern Sardinia

In north Sardinia, a polyphase ductile deformation has been distinguished by

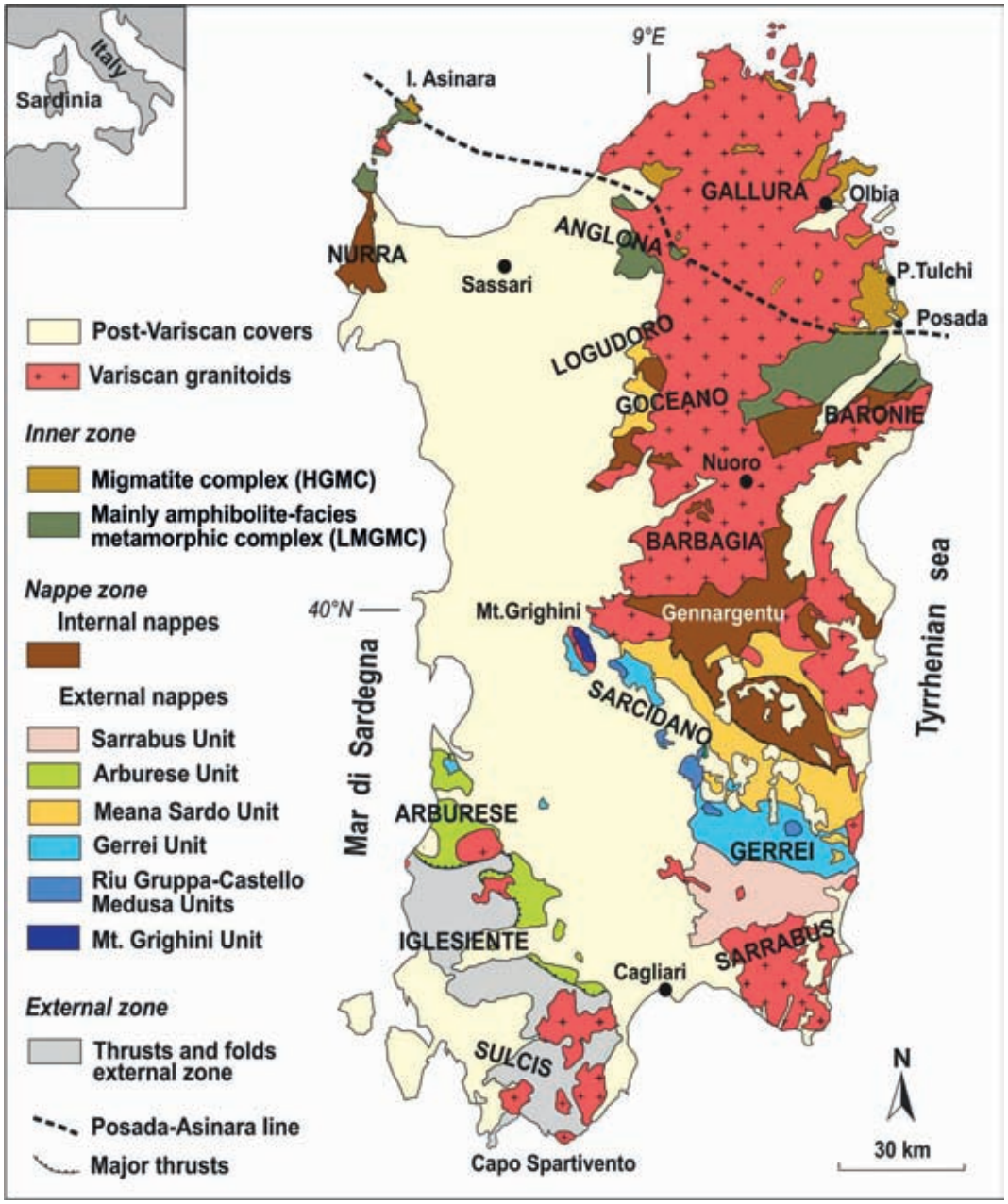

Figure 1. Tectonic sketch map of the Variscan Belt of Sardinia (modified from Carmignani et al., 2001).

Carmignani et al. (1979), Franceschelli et al. (1989), and Carosi et al. (2005 and references therein). The oldest D_1 collision-related deformation phase is well-recorded in the low-grade metamorphic rocks of the L-MGMC, especially in the southern portion of the Nurra-Asinara transect, where it is associated with the development of a penetrative S_1 axial plane foliation of SW-facing folds (Carmignani et al., 1979; Franceschelli et al., 1990; Simpson, 1998; Carosi and Oggiano, 2002; Montomoli, 2003; Carosi et al., 2004a). Late D_1 ductile/brittle shear zones, showing a top to the SW sense of movement, overprint F_1 folds. Moving to the northernmost part of the study sections, we can progressively observe the complete transposition of sedimentary bedding and S_1 foliation by the D_2 phase, meaning that S_1 is only recognized on the microscopic scale in D_2 microlithons or as inclusion trails in post-D_1 Barrovian porphyroblasts such as: plagioclase, biotite, garnet, staurolite and kyanite.

Helbing and Tiepolo (2005) attributed all pre-D_2 minerals crystallised during the M_1 event to a pre-Variscan basement in NE Sardinia intruded by late orogenic Ordovician granitoids and overlain by a cover with interlayered Middle-Ordovician acidic igneous rocks. On the contrary, Franceschelli et al. (1982a; 1982b), Elter et al. (1986) and Carosi and Palmeri (2002) attributed D_1 deformations of the low- to medium-grade metamorphic rocks of NE Sardinia to Variscan orogeny.

The D_2 deformation phase is associated with the development of upright up to NE verging folds and dextral shear zones. The large shear belt (former Posada-Asinara Line) that divides the HGMC to the north from the L-MGMC to the south, developed during the D_2 tectonic phase. The NW-SE trending shear belt is interested by an important dextral shearing that crosscuts the entire Sardinian branch of the southern Variscan Belt from west to east. Several new results have been obtained by structural and kinematic studies of the Posada-Asinara Line in the last few years (Carosi and Palmeri, 2002; Iacopini et al., 2008; Carosi et al., 2005; 2009; Frassi et al., 2009; Carosi et al., 2012):

1) A sinistral top-to-NW shear belt that originated during the start of the D_2 phase in the HGMC was observed in the central part of northern Sardinia (Carosi et al., 2012).

2) A dextral top-to-SE shear belt developed brittle and brittle to ductile mylonites during the D_2 phase within both metamorphic complexes of the Inner zone.

3) High-strain phyllonites mark the boundary between the two metamorphic complexes, while low-strain phyllonites in the HGMC, involving bodies of sinistral mylonites and mm-thick cataclasites, overprint previous phyllonites and mylonites. The field relationships reveal that the D_2 sinistral shearing anticipated the dextral tectonic movements. The D_2 deformation phase is associated with a non-coaxial flow with an instantaneous contribution of pure and simple shear (Carosi and Palmeri, 2002; Iacopini et al., 2008, 2011; Frassi et al., 2009; Carosi et al., in press). The D_2 transpressional deformation may be connected to the NNE-SSW compression and the NW-SE shear displacement (Carosi and Oggiano, 2002; Carosi and Palmeri, 2002; Carosi et al., 2004a; 2005; 2009; Iacopini et al., 2008). The continuous and heterogeneous D_2 deformation phase generated even tighter NE-verging F_2 folds in a northwards direction towards the Posada-Asinara Line and a dextral shear that becomes prevalent in the high-strain zone. The D_2 transpression phase shows a crustal scale shear deformation that overprinted previous D_1 structures that are referable to the nappe stacking and the top-to-S and SW thrusting. The predominant L_2 mineral lineation suggests an orogen-parallel extension and the change of the tectonic transport from the D_1 to the D_2 phase.

The likely position of Sardinia as attached to the NE sector of the Cantabrian indenter could

explain the orogen-parallel extension during the genesis of the Ibero-Armorican arc (Conti et al., 2001; Carosi and Oggiano, 2002; Carosi and Palmeri, 2002). Alternative explanations for the orogen-parallel extension can be sought in the general progressive curvature of the belt or in the presence of an irregular collisional margin. The D_1 phase probably developed during the start of frontal collision, while the D_2 deformation is the product of the growing effect of the horizontal and orogen-parallel displacement during the increased curvature of the belt stage (Carosi et al., 2004b; Iacopini et al., 2008). Furthermore, a switch in the attitude of the L_2 mineral lineation moving from the southern to the northern sectors has been identified. The L_2 lineations are variable from almost sub-horizontal and parallel to A_2 fold axes in the southern part of Asinara Island to down-dipping in its northern part. This is in agreement with the theoretical models proposed for transpression by Tikoff and Teyssier (1994). A D_3 deformation phase forming upright metric to decametric open folds developed subsequently. F_3 folds are associated with an S_3 axial plane crenulation cleavage. The D_4 tectonic phase is revealed by metric to decametric folds with sub-horizontal axial planes.

Timing of the D_1 and D_2 deformations

Microstructural relationships, microprobe analyses and $^{40}Ar/^{39}Ar$ laser probe analyses of white micas led Di Vincenzo et al. (2004) to better define the age of the S_1 and S_2 foliation in the garnet zone of the Baronie area and define more precisely the ages of the collisional (D_1) and transpressional (D_2) phases. Syn-D_1 celadonite-rich white mica inside plagioclase in the garnet zone allowed these authors to date the S_1 foliation at 330-340 Ma. The D_2 ages are restricted to ~ 320-315 Ma. The results of U-Th-Pb ages obtained from zircons and monazites collected from sinistral and dextral shear zones reveal that the shear zones have been active since 320 Ma (Carosi et al., 2012). The relationships between the tectonic deformations reveal that the sinistral shear zones were active before the dextral ones during the transpressional phase, and caused the early exhumation of the HGMC and its oblique transport above the L-MGMC (Carosi et al., 2012). The chronological relationships between the sinistral and dextral shear zones are not fully clarified by the U-Th-Pb geochronological data and related analytical errors. The shear zones active in a transpressive context in the range 320-310 Ma, as first elucidated by Carosi and Palmeri (2002), are now considered to be a typical feature of the southern branch of the Variscan Belt (Schneider et al., 2014 and references therein). The age of 320 Ma ascertained for the dextral shear zones in the HGMC from southern Corsica is in perfect agreement with the age of the D_2 phase in N Sardinia (Giacomini et al., 2008; Carosi et al., 2012), confirming the well-known and accepted close geological, structural and geochronological kinship between southern Corsica and northern Sardinia.

Variscan metamorphism and the deformation of selected transects

NW Sardinia (Nurra-Asinara region)

The northwestern-most portion of the Sardinian Variscan basement crops out in the Nurra-Asinara region (Figures 2, 3). From southern Nurra to the north of Asinara Island, we pass from the L-MGMC to the HGMC, both of which are intruded on by late Variscan granitoids (Carmignani et al., 1979; Carosi and Oggiano, 2002; Carosi et al., 2004a; Iacopini et al., 2008; Franceschelli et al., 2005a; Rossi et al., 2009). The L-MGMC crops out in Nurra and southern-central Asinara. It comprises phyllite (Figure 4a), black phyllites, oolitic ironstone (Franceschelli et al., 2000), metavolcanite, metabasite, metasandstone and

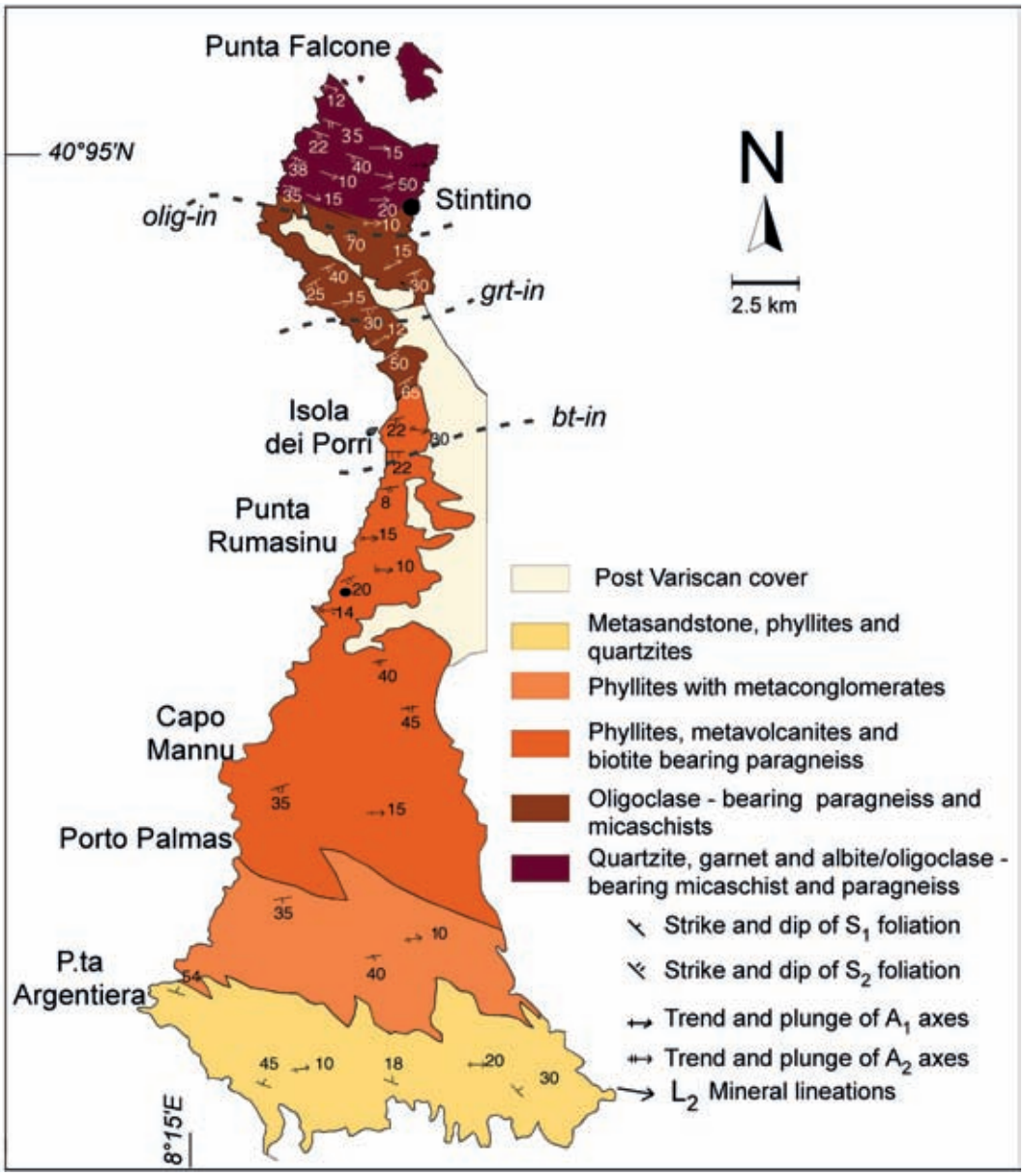

Figure 2. Geological sketch map of the Nurra peninsula (modified from Iacopini et al., 2008). Mineral abbreviations as in Fettes and Desmons (2007). Olig: oligoclase.

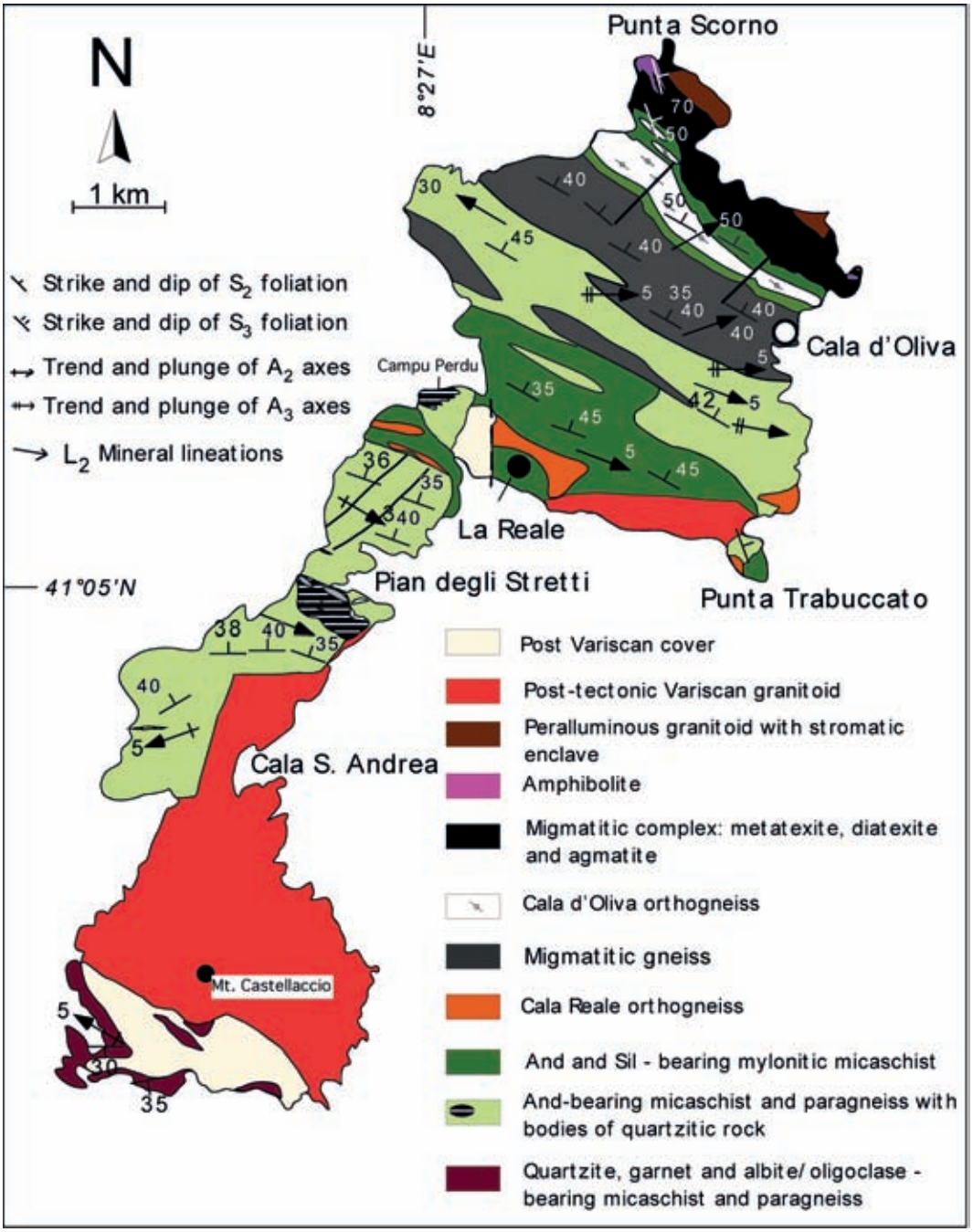

Figure 3. Geological sketch map of Asinara Island (modified from Carosi et al., 2004a).

Figure 4. Structures at the outcrop scale in the Nurra-Asinara section. a) Type 3 interference pattern of F_1 and F_2 folds in Silurian black shale in the Argentiera area, southern Nurra. The F_1 folds are tight and recumbent, and affected by upright F_2 folds showing a sub-vertical spaced crenualtion cleavage. The width of the view is nearly 20 cm; b) contractional top-to-the-SW D_1 ductile/brittle shear zone in Silurian black shale in Porto Palmas, southern Nurra. The cm-scale S-C fabric is the main kinematic indicator; c) tight F_2 folds in alternating quartzite and shale layers with similar geometry, central Asinara. The F_2 folds have a northern vergence; d) foliated migmatites in the northernmost portion of Asinara Island showing boudins of dark amphibolites and the intrusion of post-tectonic pegmatite dykes; e) cm- to dm-size late tectonic andalusite crystals in micaschists and quartzites of central Asinara Island, Stretti area; f) Augen feldspar crystals in Punta Scorno orthogneiss, northern Asinara. Asymmetric sigma-type tails point to a top-to-the-SW sense of shear that is interpreted as evidence of the overthrusting of the HGMC onto the L-MGMC.

quartzite in the south of Nurra, followed by paragneiss, micaschist, subordinated quartzite and micaschist in central Nurra, and garnet and oligoclase-bearing paragneiss in north Nurra and in the southern sector of Asinara Island (Carmignani et al., 1979; Carosi and Oggiano, 2002; Iacopini et al., 2008) (Figure 3).

In central Asinara, the L-MGMC is represented by late-tectonic andalusite (Figures 4e; 5b), sillimanite-bearing porphyroblastic paragneiss and micaschist (Figure 5a), quartzite, amphibolite, orthogneiss and augen gneiss, and fibrolite, andalusite and cordierite-bearing mylonitic micaschist (Figure 3). The HGMC cropping out in the north part of Asinara Island consists of migmatite and migmatitic orthogneiss (Figure 4f), which is mainly composed of diatexite and metatexite with sillimanite + alkali-feldspar + cordierite, orthogneiss and banded amphibolite, sometimes included as boudins in the migmatite (Figure 4d). The L-MGMC and HGMC are separated by a tight belt of mylonitic micaschist and mylonitic orthogneiss with amphibolite boudins. The D_1 collisional event is well-recorded in the L-MGMC of south and central Nurra, and is associated with a pervasive S_1 axial plane foliation of metre to decametre SW-facing folds (Figure 4a) (Carmignani et al., 1979; Franceschelli et al., 1990; Simpson, 1998; Carosi and Oggiano 2002; Montomoli, 2003; Carosi et al., 2004a). S_1 foliation is defined by the syn-kinematic crystallization of quartz, muscovite, paragonite, albite, chlorite and oxides (Carmignani et al., 1979) (Figure 6a). In southern Nurra, the F_1 folds are metres to decametres in size and have variable opening angles (from 30° - 40° up to isoclinal). They have thickened hinges and stretched limbs, and commonly belong to Ramsay's class 2 (1967). Late D_1 ductile/brittle shallowly-dipping shear zones have been recognized in phyllites and quartzites (Simpson, 1998; Montomoli, 2003). Shear planes strike from N130 to N150 and dip 30-40° to the NE. The C-S fabric indicates a top-to-the S and SE sense of shear (Figure 4b). The shear zone, which is deformed by an

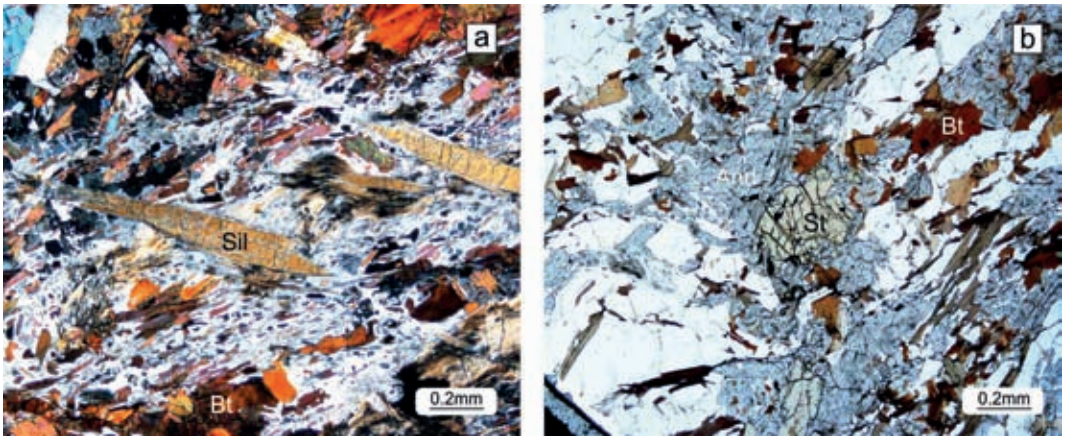

Figure 5. a) Microscopic aspect of main foliation in schists in central-north Asinara. Two different growing steps of sillimanite can be recognized: syn-tectonic fibrolitic sillimanite crystallizes along the main foliation (S_2), while prismatic sillimanite crystals are discordant and show a post-tectonic relation with the main foliation; b) microscopic relations between staurolite and late andalusite growth in schists from central Asinara. Crossed polars photomicrographs.

S_2 crenulation cleavage, is characterized by abundant sigmoidal quartz veins, which are derived from dehydration reactions during prograde metamorphism (Simpson, 1998). According to Montomoli (2003), during their development, the host rocks experienced a lowering pressure with respect to the peak metamorphic conditions estimated for the D_1 tectonic phase (Franceschelli et al., 1989; 1990). D_1-related pressure has been estimated to 0.7-0.8 GPa by Franceschelli et al. (1990) and to 0.3 GPa by Montomoli (2003) for the late D_1 event pointing out a decreasing pressure around 0.4-0.5 GPa.

The decreasing pressure values at the time of the late D_1 shear zone activity suggest that during crustal stacking the nappe pile continued to undergo overall compression, causing the development of shear zones and allowing the exhumation of the hanging wall rocks.

Going towards the north, D_2 shows a gradual strain increase up to the complete transposition of both sedimentary bedding and S_1 foliation that is recognizable only in D_2 microlithons or as inclusion trails in post-D_1 Barrovian porphyroblasts. The D_2 tectonic phase is characterized by a heterogeneous deformation, and is partitioned into large domains alternating between prevailing folding and shearing deformation (Carmignani et al., 1979; Simpson, 1998; Carosi and Oggiano, 2002; Carosi et al., 2004a; Iacopini et al., 2008). In low strain areas to the south, the D_2 deformation is characterized by an axial plane spaced crenulation cleavage and an axial plane of E-W-trending F_2 folds (Figure 4a). Moving northwards, the strain increases, and is characterized by non-coaxial deformation. In Nurra F_2 has similar fold geometry: i) changes from open (in the south) to isoclinal (in the north), with decreasing interlimb angles, and ii) varies from class 1C to class 3 (Ramsay, 1967). In central Asinara Island, the F_2 fold geometry varies from class 1C to class 2 (Ramsay, 1967) (Figure 4c). In the areas where D_2 is characterized by non-coaxial deformation, the S_2 foliation shows a mylonitic texture with kinematic indicators pointing to a top-to-the NW sense of shear. In central Asinara, kinematic indicators are badly preserved due to the HT-LP overprint due to the Late Variscan batholith intrusions (Carosi et al., 2004a).

L_2 mineral lineation is represented by both mineral grain and aggregate lineations trending parallel to the F_2 fold axes before plunging a few degrees towards the NW and SE and switching from sub-horizontal to down dipping in North Asinara. Meanwhile, the S_2 foliation maintains the same attitude. This kinematic behaviour has been interpreted by Iacopini et al. (2008) as evidence of the increasing component of pure shear in the deformation moving to the north.

In the northern part of Asinara Island, it is possible to observe the thrusting of the HGMC onto the L-MGMC. Here, in Punta Scorno, orthogneiss and kinematic indicators point to a top-to-the SW sense of shear (Figure 4f). A D_3 ductile deformation is associated with upright metric to decametric open folds and with an S_3 axial plane crenulation cleavage.

The metamorphic zoning of the Nurra region has been thoroughly examined by Carmignani et al. (1979, 1982b) and Franceschelli et al. (1986, 1990). Alternating quartzitic and micaceous layers characterize the chlorite zone, whose mineral assemblage is made up of K-Na white mica, albite, chlorite and chloritoid in variable proportions. Carbonates, epidote, iron-titanium oxides and graphite are the accessory minerals. Going northwards, a S_2 foliation gradually replaces and transposes the S_1 fine continuous foliation (Figure 6a). Inclusion trails parallel to the relict S_1 foliation that is now oriented discordantly with respect to the prevalent S_2 foliation are still preserved in albite porphyroblasts.

S_2 crenulation is ubiquitous in the northernmost part of the chlorite zone (Figure 6a). A broad range of Si a.p.f.u. characterizes

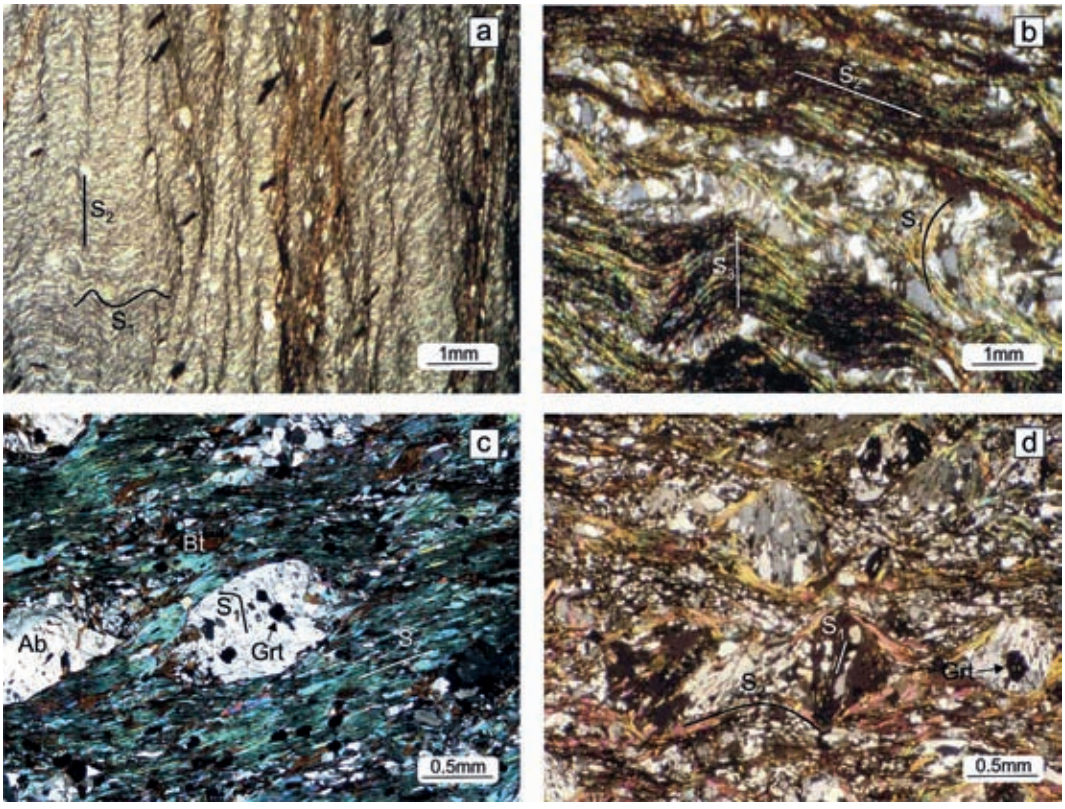

Figure 6. Microstructural features of metamorphic rocks from Nurra, NW Sardinia. a) S_1 foliation crenulated by the S_2 schistosity in micaschist; the opaque mineral grains are ilmenite; sample from chlorite zone; b) alternated phyllosilicate-rich and quartz-feldspathic layers in a metapsammite; biotite zone; c) albite porphyroblast in a phyllosilicate and garnet-rich matrix; garnet zone; d) albite porphyroblasts preserving an S_1 foliation; the porphyroblasts are surrounded by a matrix in which the S_2 foliation is identified by the alignment of phyllosilicates; garnet zone. All the photomicrographs, except (a), are in crossed polars.

the S_1 muscovite from maximum values of 6.65-6.70 in metarhyolites to minimum values of 6.07-6.20 in Al-rich rocks. As regards the biotite zone, Carmignani et al. (1982b) ascertained that the bulk composition of the rock may have an influence on the incoming of the biotite in the prograde sequence. Low Al content anticipates the first appearance of biotite, while high Al content delays its initial emergence.

The garnet zone, which is characterized by the first appearance of almandine-rich garnet, shows the assemblage albite, oligoclase, garnet, muscovite, biotite, chlorite and subordinated chloritoid. A gradual deformation of the S_1 foliation during the D_2 phase is testified by inclusion trails observed within the albite porphyroblasts (Figures 6 c,d) that appear: rectilinear, slightly to strongly-folded and, in some cases, characterized by two orientations. In the upper garnet zone, the albite porphyroblasts are surrounded by oligoclase rims.

In a first, pioneering piece of work, Ricci

(1972) suggested that Asinara Island underwent the same Barrovian metamorphism as northern Sardinia during the first Variscan phase, as indicated by the occurrence of albite-oligoclase, garnet, K-feldspar, sillimanite and relict staurolite as the main metamorphic minerals, even if the strong recrystallization of both post-tectonic HT-LP minerals (i.e. andalusite and sillimanite) tends to obliterate the previously recrystallized minerals (Figures 5 a,b). Confirmation of this hypothesis was provided by the discovery of kyanite relics replaced by sillimanite within the melanosomes of the Punta Scorno migmatite (Oggiano and Di Pisa, 1998). The fine-grained and porphyroblastic paragneisses are made up of quartz, oligoclase, garnet, biotite, white mica plus epidote, monazite, zircon and oxides. Andalusite- and sillimanite-bearing paragneisses and micaschists are characterized by remarkable modal contents of andalusite, an abundance of relict garnet, and staurolite (Figure 5b), which is replaced by a mineral assemblage consisting of andalusite, biotite and oxides, with accessory minerals like tourmaline, ilmenite, apatite and zircon. The amphibolites are made up of hornblende and plagioclase and minor contents of biotite, chlorite and Fe-Ti oxides. They show a previous granulite stage that is revealed by the occurrence of Ca-clinopyroxene and garnet relics. Worthy of note is the survival of Barrovian assemblages, which are pre- to syn-kinematic as to the D_2 deformation. This is despite the general HT-LP metamorphism that has been hypothesized by the authors examining Asinara Island to have been an Abukuma-type HT-LP metamorphism (Figure 4e).

North central Sardinia

In the Goceano area, the northernmost strand of the Nappe zone crops out in a narrow N-S trending belt (Oggiano, 1994) (Figure 1). The area is characterized by the superposition of the L-MGMC (Fiorentini Unit) over the outer nappes (Ozieri Unit). The former is made up of metasiltites, metasandstones and quartzites, while the latter comprises metasandstones, metasiltites, metavolcanics, black schists and marbles attributed to the classical Cambrian to Devonian sequence of the Nappe zone. Both tectonic units are affected by a syn-collisional low-grade regional metamorphism, and by a late HT-LP amphibolitic overprint (andalusite/sillimanite, cordierite, oligoclase and biotite: Casini and Oggiano, 2008).

The deformation history is typical of the internal units of the Nappe zone (Carosi and Pertusati, 1990; Carmignani et al., 1994; Carosi et al., 2004c), with S_2 sub-horizontal foliation transposing a former S_1 penetrative foliation, both of which are associated with S and SW-verging overturned F_1 and F_2 folds. Millimetre-scale-size albite porhyroblasts are mostly intertectonic compared to the S_1 and S_2 foliations, showing the same relationships as the albite porhyroblasts in the northern outcrops of the L-MGMC.

The nappe pile is affected by large-scale F_3 antiforms and synforms with mainly NW-SE trending axes. The antiforms are later affected by collapse folds and low-angle normal faults (Lanfs) (Casini and Oggiano, 2008). The Lanfs show a top-down-to-NE sense of shear on the NE limbs of the F_3 antiforms, and a top-down-to-the SW sense of shear on the SW limbs of the antiforms.

The peculiar feature of the Goceano area is the link between HT-LP metamorphism and the Lanfs, because some HT-LP minerals (such as andalusite and oligoclase) are affected by the deformation connected to the Lanfs. Casini and Oggiano (2008) related the latest tectonic stages to a core-complex style of exhumation.

In Anglona and SW Gallura, the transition from the L-MGMC to the HGMC is highlighted by a narrow phyllonitic belt striking nearly NW-SE and dipping to the NE. It is worthy of note that, unlike the Baronie area, the HGMC here overthrusts the L-MGMC. Field mapping,

micro- and meso-scopic structural analyses, and a detailed tectonic reconstruction based on relationships between metamorphic mineral growth and deformation have been carried out in the last ten years (Carosi et al., 2005; 2009; 2012).

The L-MGMC comprises a metasedimentary sequence that is mainly represented by metre-scale thick layers of micaschists and paragneisses, with sporadic thin layers of quartzite, and crops out in the southwestern sector of the Gallura region and Coghinas Lake area (Figure 7).

In the northern outcrops, we can observe a SW–NE increase in the metamorphic grade of the Barrovian metamorphism from the biotite- up to the kyanite-biotite zone over less than 2 km. This is a consequence of ductile shearing in a transpressional regime (Carosi and Palmeri, 2002; Carosi et al., 2009; 2012). Centimetre-scale-size porhyroblasts of kyanite and staurolite, which have been deformed and retro-metamorphosed, have been found near to the phyllonitic belt (Figure 8a), where a 100 m-thick amphibolite lens with relics of eclogitic assemblages has also been documented (Oggiano and Di Pisa, 1992; Cortesogno et al., 2004; Cruciani et al., 2015). The boundary between the eclogitic body and the micaschists is highlighted by a gradual reduction in the amphibole content, a reduction in the crystal size and an increased shape preferred orientation (SPO) of the amphiboles. The lower boundary of the eclogitic lens is defined by a metric-thick quartz-feldspathic layer with a mylonitic fabric containing centimetre-sized eclogitic lenses and several inclusions with centimetre-scale euhedral crystals of garnet.

Small bodies of diatexites, with agmatite and nebulite structures, and hornfelses have been locally found in the Coghinas Lake area (Oggiano and Di Pisa, 1992). In the same area, stretched amphibolitic bodies and decimetre-size trondhjemitic leucosomes with centimetre-scale cordierite nodules have also been detected (Carosi et al., 2009).

The phyllonitic belt shows a variable thickness from 50 m up to 250-300 m. Although the phyllonitic matrix has a homogeneous, reduced grain size, centimetre-scale lenses have been locally observed with < 2 mm-size preserved, rounded porphyroclasts of plagioclase.

The HGMC crops out in the northeastern part of the study area, and is characterized by deep weathering that often masks the migmatitic texture. Metatexites are the dominant lithotype with minor amounts of augen migmatitic gneisses and garnet-bearing orthogneisses. Few thin melanocratic layers have been detected around the thicker leucosomes that have a granitic or trondhjemitic composition, whereas rare homogeneous diatexites (nebulitic structures) are present in the northern portion of the complex. The southeastern part of the complex is characterized by abundant metre- and centimetre-scale pegmatites. Foliated granitoids, interpreted as the precursor of the post-Variscan batholith (Di Pisa and Oggiano, 1987; Macera et al., 1989), crop out in NE areas.

Mylonitic fine-grained gneisses with a sillimanite-muscovite mineral assemblage and centimetre-scale quartz-feldspathic boudins, mylonitic pegmatite veins and mylonitic quartzites crop out in two narrow belts striking NNW-SSE. On the east side of the phyllonitic belt, metric-sized bodies of migmatitic gneiss and metre-scale thick leucocratic quartz-plagioclase bands developed parallel to the main foliation. Moving towards the phyllonitic belt as the non-coaxial deformation increases, the thickness and frequency of quartz-feldspathic pegmatitic veins are progressively reduced, and near the phyllonitic belt only small and rare feldspar-rich layers have been preserved.

Relicts of the D_1 deformation phase have been preserved only in the southern portion of the L-MGMC, and were transposed by the D_2 deformation phase. D_2 deformation produced a

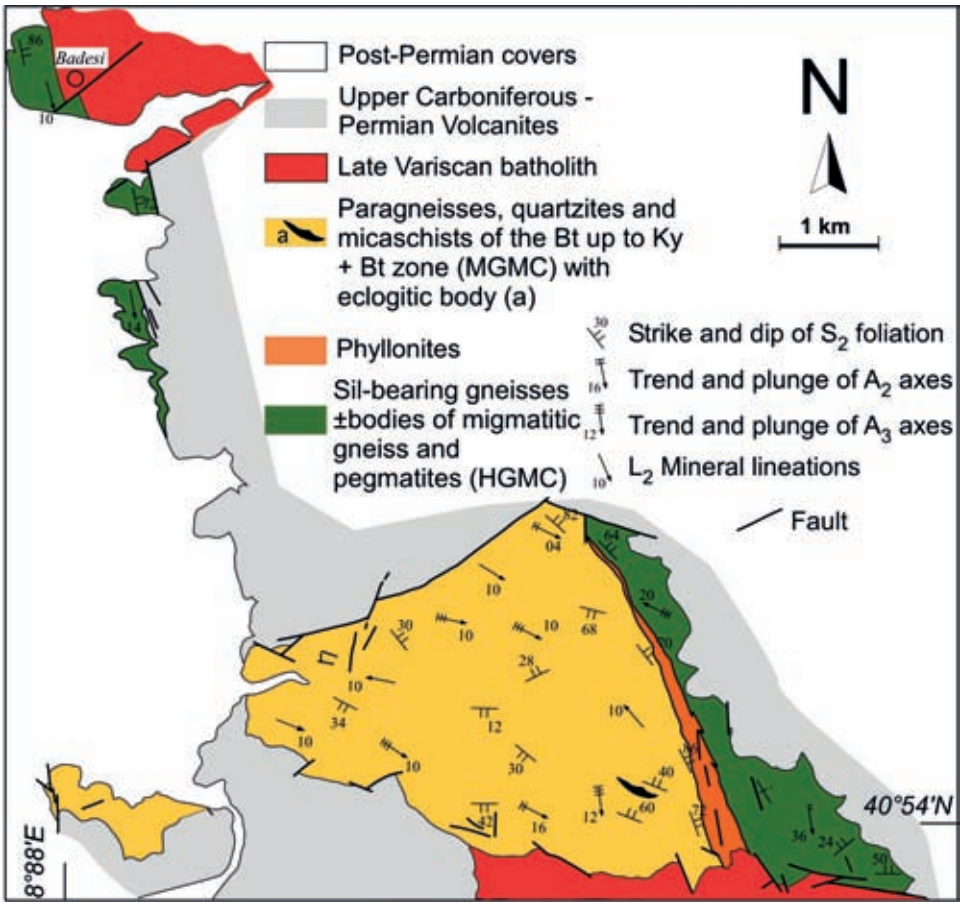

Figure 7. Geological sketch map of the Anglona-southern Gallura region (modified from Carosi et al., 2012).

pervasive S_2 foliation, F_2 folds and L_2 mineral lineation (Carosi et al., 2009). The interlimb angle and the geometry of the F_2 folds testify to an increase in the D_2 finite strain traced from W-SW towards the phyllonite belt. Open folds were documented in the southern less-deformed portions, whereas isoclinal folds with stretched limbs and locally isolated fold hinges were documented approaching the phyllonite belt (Figure 8b). The S_2 foliation shows a variable dip, becoming steeper near the phyllonites. The L_2 mineral lineation usually plunges less than 25° either towards the NW or SE.

The D_2 high-strain deformation defines a narrow shear belt characterized by two different superposed kinematics in an overall transpressional setting: i) a first sinistral top-to-the-NW shear sense developed in the HGMC, with a more prominent down-dip component of the deformation, and ii) a second dextral top-to-the-SE shear sense developed heterogeneously in the L-MGMC, with a prominent strike-slip component of deformation (Carosi et al., 2005; 2009; Frassi et al., 2009). The sinistral shear zones, with clear kinematic indicators, are cross-cut by dextral shear zones (Carosi et al.,

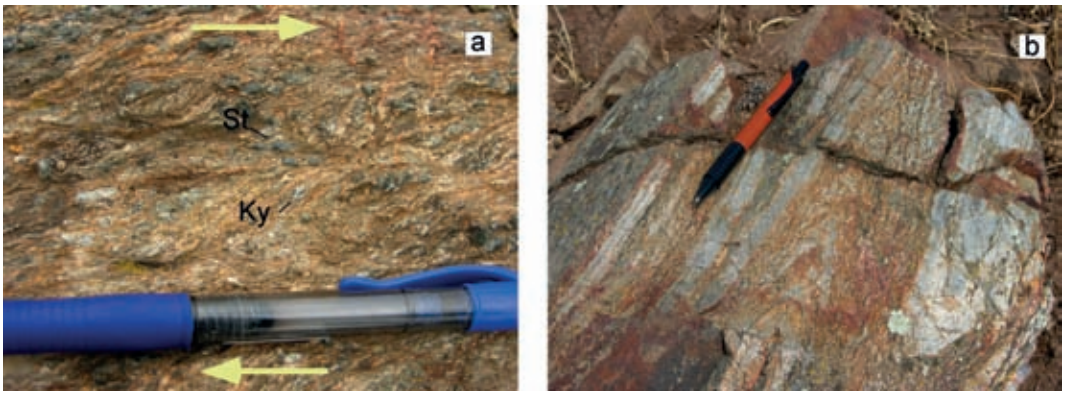

Figure 8. a) Cm-size staurolite and kyanite crystals and shear band cleavage in micaschists in the L-MGMC, Tungoni area, Anglona (the arrows highlight the dextral sense of shear); b) F_2 intrafoliar, isoclinal folds in kyanite-bearing micaschists and quartzites in the L-MGMC, Tungoni area, Anglona.

2009; Frassi et al., 2009).

The dextral shear belt remained active until exhumed to upper crustal levels, where phyllonites and a network of thin cataclasites initially overprinted both early phyllonites and sinistral mylonite. A kinematic assessment of the flow using a stable porphyroclast analysis and the quartz c-axis highlighted a non-coaxial flow with a change from simple-shear dominated transpression during sinistral shearing to a pure shear dominated transpression during the dextral shearing (Carosi et al., 2005; Frassi et al., 2009). During this second stage, the dextral shear deformation occurred under a pure-shear-dominated regime that enhanced the extrusion of the HGMC and produced a telescoping of the Barrovian isograds that in map view is marked by a condensed transition within 2 km from biotite- to biotite + kyanite zones (Carosi and Palmeri, 2002; Carosi et al., 2009; Frassi et al., 2009).

A U-Th-Pb analysis of zircon and monazites allowed to assess the age of the D_2 shearing as 320-310 Ma (Carosi et al., 2012). Even though the superposition relationships enabled us to examine the overprinting of the dextral mylonites on the sinistral ones, the detected age did not allow us to clearly discriminate between the two events. Two later phases of deformation affected the D_2 mylonitic belt, producing large-scale folding (Carosi et al., 2009).

The temporal variation in kinematics, flow type and finite strain documented in this area may be explained by a regional change in the stress field during the post-collisional, orogen-parallel displacement of the continental margins caught up in the Variscan orogeny. The change from sinistral to dextral kinematics, which joined a change in flow type, implies that the regional stress field may have rotated c. 90° from W-SW-E-NE to S-SW-N-NE during the post-collisional exhumation stage (Frassi et al., 2009).

NE Sardinia

Low- to Medium-Grade Metamorphic Complex. As in the other sections of the Variscan basement of Sardinia, the D_1 deformation has produced prominent structures in the southwestern area, where a pervasive low-grade S_1 foliation can be observed in the field. S_1 strikes NE–SW and dips 40-50° to the SE. The A_1 fold axes trend nearly E-W, plunging a few degrees both to the west and the east.

The S_1 foliation, defined by the orientation of muscovite, paragonite, chloritoid, quartz and Fe-oxides in microlithons, is a fine, continuous foliation in the more pelitic layers and a spaced foliation in the more psammitic ones.

A few kilometres south of the village of Lula (Figures 9, 10), the S_1 foliation is affected by tight F_2 folds with steeply-dipping axial planes and NE vergence. Axial plane S_2 foliation is a discrete crenulation cleavage (classification according to Passchier and Trouw, 2006). The S_2 foliation strikes NW-SE and dips 40-50° to the SW. The A_2 fold axes trend ~ NE-SW with variable plunge. The S_2 foliation domains are from rough to smooth and are mainly due to the reorientation of the S_1 syn-kinematic minerals. We only sometimes observed a crystallization of biotite, chlorite and white mica parallel to S_2 in the southern areas. Moving to the north, the S_2 foliation becomes much more penetrative and, at the same time, the spacing between the foliation domains progressively decreases. Dynamic recrystallization is much more evident, and the thickness of the foliation domains increases approaching the orthogneisses in the north (Figure 10). Starting from the chloritoid-bearing schists, the S_2 foliation is pervasive and becomes increasingly prominent until it completely transposes the S_1 foliation planes. The S_1 foliation can be recognized only as inclusion trails in garnet porphyroclasts that are discordant with respect to the external S_2 foliation and in microlithons. The S_2 foliation domains are anastomosing around porphyroclasts that are mainly represented by garnet. An S_3 spaced crenulation cleavage affects the S_2 foliation. This cleavage is related to later open steep to upright antiforms and synforms on a cm to a km-scale. Starting from a few km north of Lula, a component of dextral shearing began to develop in metre-thick levels. Approaching Posada Valley, the S_2 foliation transposed the S_1 foliation and shearing became the most important component of the D_2 deformation. The L_2 mineral lineation becomes prominent as the shearing increases, trending nearly N070E-N080E. A dextral sense of shear is detected by a variety of shear sense indicators, especially mica-fishes, C-S fabrics and sigma-type porphyroclasts. C foliation is common in the albite-bearing micaschists (Carosi and Palmeri, 2002; Carosi et al., in press).

In the southern part, the D_2 deformation is characterized by nearly upright to N and NE verging folds, pointing to a SE-NW directed shortening (Figure 11a). As deformation increases to the north, the D_2 deformation is progressively marked by an increasing shearing component, becoming prominent approaching the Ordovician orthogneisses to the north (Figure 10) (Carosi and Palmeri, 2002). The shearing is increasingly salient starting from the reverse limbs of the F_2 folds, where the strain has concentrated. The area is affected by an overall transpressional deformation characterized by a large component of pure shear associated with simple shear (Carosi and Palmeri, 2002). Dextral shearing is the prominent deformation in both the micaschist and gneiss up to the southern boundary of the HGMC along Posada Valley. The steeply-dipping attitude of S_2 foliation caused by transpression has been affected by open symmetrical folds with sub-horizontal axial planes, named “collapse folds”. This suggests sub-vertical shortening and sub-horizontal extension.

The metasedimentary sequences of NE Sardinia are characterized by a telescoping of the metamorphic isograds from biotite to sillimanite + K-feldspar zones in a very restricted area of only few dozen kms (Franceschelli et al.,1982a; Elter et al., 1986), which is due to intense shearing in a transpressional regime (Carosi and Palmeri, 2002; Carosi et al., 2008).

The key minerals of the metamorphic zones from south to north are: i) biotite; ii) garnet; iii) staurolite + biotite; iv) kyanite + biotite; and v) sillimanite + K-feldspar (Figures 9, 10). The

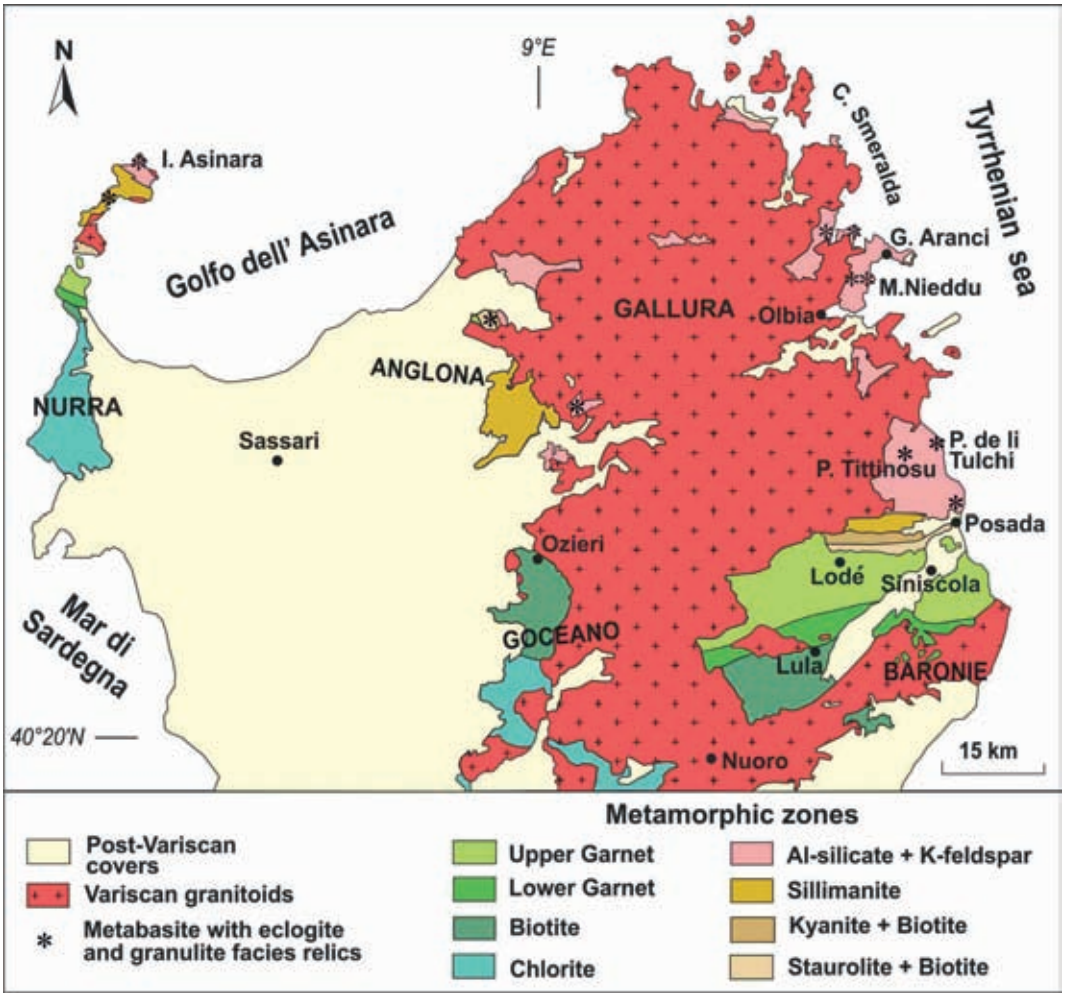

Figure 9. Metamorphic zonation in metapelitic and metapsammitic rocks from the Variscan basement of northern Sardinia, (from Franceschelli et al., 1982a, 2005a modified). The main outcrops of metabasite with eclogite and granulite facies relics are also shown.

garnet zone is further subdivided into garnet + albite and garnet + oligoclase sub-zones (Franceschelli et al., 1982a).

The biotite zone is mainly characterized by the following assemblages: quartz, albite, muscovite, biotite, chlorite, ± K-feldspar. Locally, the sedimentary bedding, as well as other sedimentary remains, such as fining upwards and erosional contacts (Figure 11a), are still recognizable south of Lula village (Franceschelli et al., 1982b; Ricci et al., 2004; Costamagna et al., 2012). The S_1 foliation is preserved in microlithons that are partially overprinted by D_2 (Figure 13a). The albite porphyroblasts sometimes include graphite helicitic inclusions.

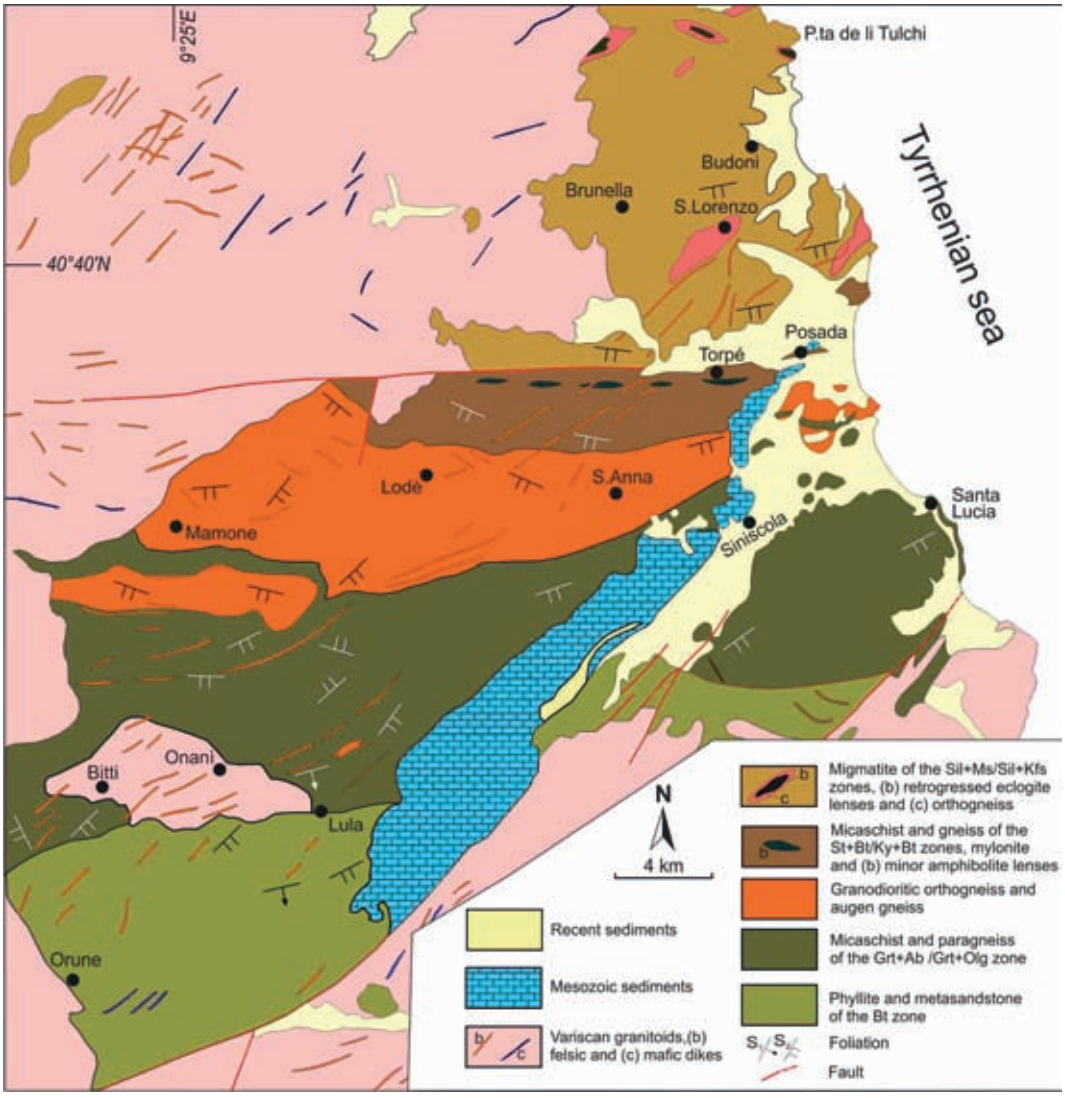

Figure 10. Geological sketch map of NE Sardinia (modified from Carmignani et al., 2001).

Almandine-rich garnet coexisting with biotite, chlorite, quartz, albite-oligoclase, muscovite and, locally, chloritoid is the main assemblage of the garnet zone. The S_1 minerals are quartz, muscovite and chlorite, and are frequently found as oriented inclusions (Figure 13b), while garnet and chloritoid are post-D_1, pre-D_2 phases. According to Helbing and Tiepolo (2005), the garnet in the lower garnet zone (i.e. garnet + albite zone of Franceschelli et al., 1982a; 1982b) is a pre-Variscan relict, whereas the albite derives from Variscan metamorphism. These authors suggest a metamorphic "jump" from biotite to the garnet zone, marking the cover

Figure 11. a) Mesoscale folding in the biotite zone consisting of an S_1 foliation nearly parallel to sedimentary bedding, both folded by F_2 folds in metasandstone. The outcrop locality is a few kilometres south of Lula, NE Sardinia; b) centimetric staurolite porphyroclasts (arrows) along the S_2 foliation of staurolite + garnet schists. Outcrop locality: Bruncu Niedddu (staurolite+biotite zone); c) centimetric, bluish kyanite crystal along the mylonitic foliation in the staurolite + garnet schists of the Bruncu Nieddu locality (kyanite+biotite zone); d) alternation between fibrolite-rich (white) and fibrolite-poor layers in unmelted metapelitic greywacke belonging to the Migmatite zone. Outcrop locality: Punta Bados.

and basement contact, but field and petrological evidence of this "jump" is not provided.

The staurolite + biotite zone is characterized by the main assemblage, plagioclase, staurolite (sometimes in centimetre-sized crystals, Figures 11b, 13c), garnet and biotite. Most porphyroblasts show syn-D_1, pre-D_2 cores and, in some cases, syn-D_2 rims (Franceschelli et al., 1982a; 1982b; Carosi and Palmeri, 2002).

The kyanite + biotite zone shows kyanite, biotite, garnet, white mica and plagioclase as the typical assemblage. Elongated, centimetric-sized kyanite crystals are sometimes recognizable on the outcrop scale in the micaschist (Figure 11c). Staurolite, biotite, kyanite, garnet, white mica and plagioclase are syn-D_1, pre-D_2 minerals (Franceschelli et al., 1982b; Connolly et al., 1994).

The sillimanite zone has been mapped in Posada Valley. Both fibrolitic and prismatic

sillimanite were observed, but fibrolite strongly prevails. The rocks of this zone, near to the boundary with the kyanite + biotite zone, are characterized by a mylonitic texture, and northwards show mm-sized alternating mafic and quartz-feldspathic layers following the S_2 foliation. The main mineral assemblage is quartz, plagioclase, garnet, sillimanite, muscovite and biotite.

High-Grade Metamorphic Complex. The Migmatite Complex consists of igneous- and sedimentary-derived gneiss and migmatites (Cruciani et al., 2001; 2008a; 2008b; 2014a; 2014b), with bodies and lenses of metabasite with eclogite (Franceschelli et al., 1998; 2007; Cruciani et al., 2012) and granulite (Franceschelli et al., 2002; Cruciani et al., 2002) facies relics. Layered amphibolites resembling leptyno-amphibolite complexes have also been described by Franceschelli et al. (2005b). The paragneiss and migmatite commonly contain calc-silicate rocks and nodules and fibrolite-rich nodules (Figure 11d) (Franceschelli et al., 1991). The Migmatite Complex matches the sillimanite + K-feldspar zone of Franceschelli et al. (1982a). Sillimanite in the fibrolite variety is the most common allumosilicate; more rarely kyanite crystals and kyanite relics in plagioclase were found (Palmeri, 1992; Cruciani et al., 2001; Cruciani et al., 2014a).

Three main deformation phases (D_1, D_2, D_3) have been identified in the migmatites (Cruciani et al., 2008a). Two additional deformative phases (D_4, D_5) were recognized by Elter et al. (2010).

D_1, which is not clearly recognizable in the field, is documented by the transposition of centimetre-sized leucosomes. The D_2 phase is revealed by N140°-striking isoclinal folds with a SE dip of 2–18°. On the S_2 schistosity, three different poly-mineralogical lineations have been recognized: the oldest consists of rods and/or pencils of plagioclase+quartz; the second is a fibrolite+quartz mineralogical lineation with a N 158° strike and a SE dip of 20–30° at a 0-20° angle with the previous mineralogical lineation; and the third consists of muscovite, which sometimes overprints the fibrolite+quartz lineation. Passive, asymmetrical folds, shear-band boudins, sigma-type porphyroclasts and kinematic indicators related to the rods and pencils of plagioclase+quartz indicate a top to the NW component of the shear, while those associated with the fibrolite+quartz and muscovite (D_2 phase) lineations suggest a top to the SE/NE component of the shear. The occurrence of two opposite senses of shear (top to NW and top to SE/NE) on the same foliation surface (S_2) has been interpreted by Corsi and Elter (2006) as being due to non-coaxial D_1 and D_2 deformation events, i.e. characterized by a component of pure shear coexisting with one of simple shear. The top-to-NW shear component was probably associated with the end of compression and crustal thickening, whereas the top-to-SE/NE component derived from tectonic inversion during the exhumation of the metamorphic basement. The D_4 event shows a composite structural frame characterized by the superposition of three sub-events, in some cases with only a local distribution. The D_5 event represents the last deformational event, and is not accompanied by a distinct metamorphic episode.

According to Elter et al. (2010), the Variscan HGMC of NE Sardinia can be regarded as a NW-SE-oriented pop-up structure developed in the Late Carboniferous in a continent-continent oblique collision context. This system could lead to the exhumation of HT rocks from amphibolite facies to greenschist facies by telescoping processes coeval with the transcurrent movement.

Along the NE coast of Sardinia (north of Olbia, Figure 9), the sedimentary-derived migmatite contains 3-5 vol.% stromatic leucosomes (Cruciani et al., 2008a) (Figure 12a). The

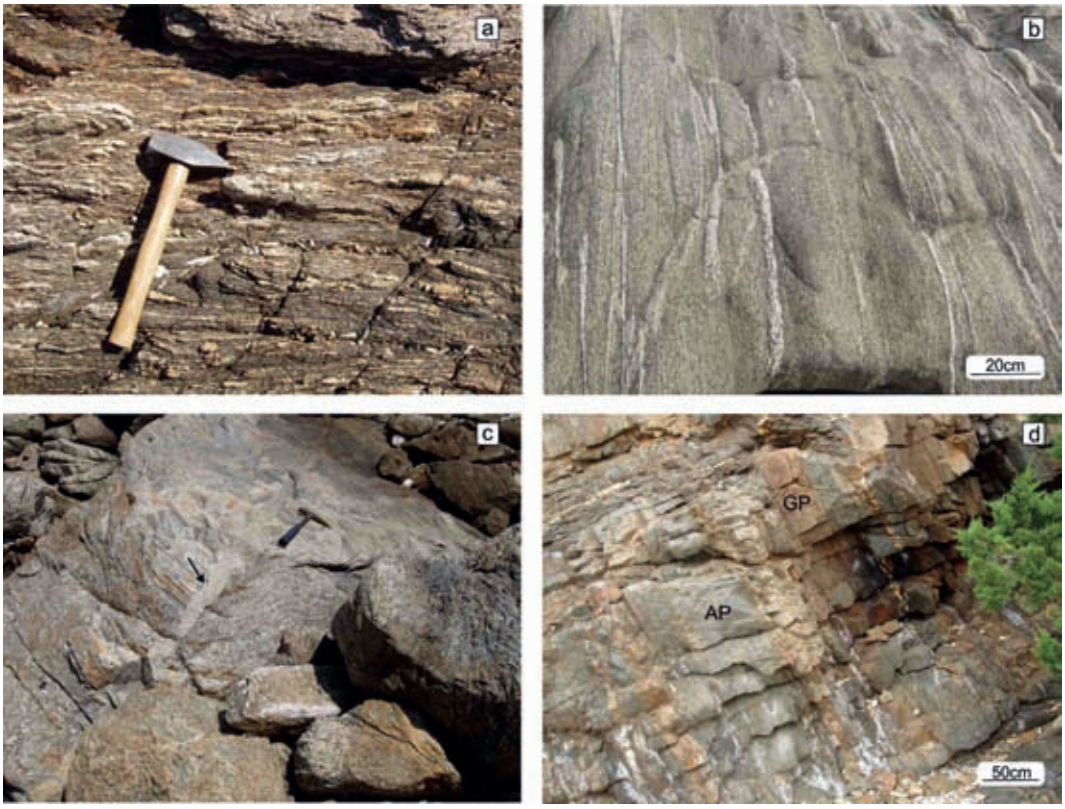

Figure 12. Field aspect of rocks belonging to the Migmatite zone of NE Sardinia: a) sedimentary-derived, Al-silicate-bearing migmatites with thin and elongated leucosomes. The migmatite as a whole has a milonytic appearance. The pervasive S_2 foliation (horizontal in the picture) is parallel to the leucosome elongation. Outcrop locality: Punta Sirenella; b) thin and elongated amphibole-bearing leucosomes surrounded by greyish mesosome. The leucosomes are parallel to the regional S_2 foliation; the black spots in the leucosomes are amphibole crystals. Outcrop locality: Punta Sirenella; c) migmatized orthogneiss crosscut by a leucogranite dyke (arrow) at the Porto Ottiolu locality; d) alternation of brownish garnet-pyroxene (GP) layers and greenish amphibole-plagioclase (AP) layers in the Punta de li Tulchi eclogite outcrop.

mesosomes consist of plagioclase (25-35%), quartz (30-40%), biotite (15-20%), ± kyanite (up to 4-5%), ± garnet (up to 2-3%), ± fibrolite (up to 20%), coarse-grained muscovite (10-20%) and zircon, with apatite, rutile and monazite as accessory phases. The leucosomes consist of quartz (40-50%), plagioclase (35-45%), biotite (≤ 5%), ± garnet (< 1%), ± kyanite (< 5%), ± fibrolite (< 10%), K-feldspar (≤ 1%) and retrograde muscovite (5-10%). The leucosomes vary in length from a few centimetres up to 1-2 m, and are deformed, stretched or folded. Discontinuous to boudin-shaped leucosomes also occur.

The rare granitic leucosomes differ from trondhjemitic ones only by the increase in the modal content of K-feldspar, up to 25%. Melanosomes, when present, are characterized

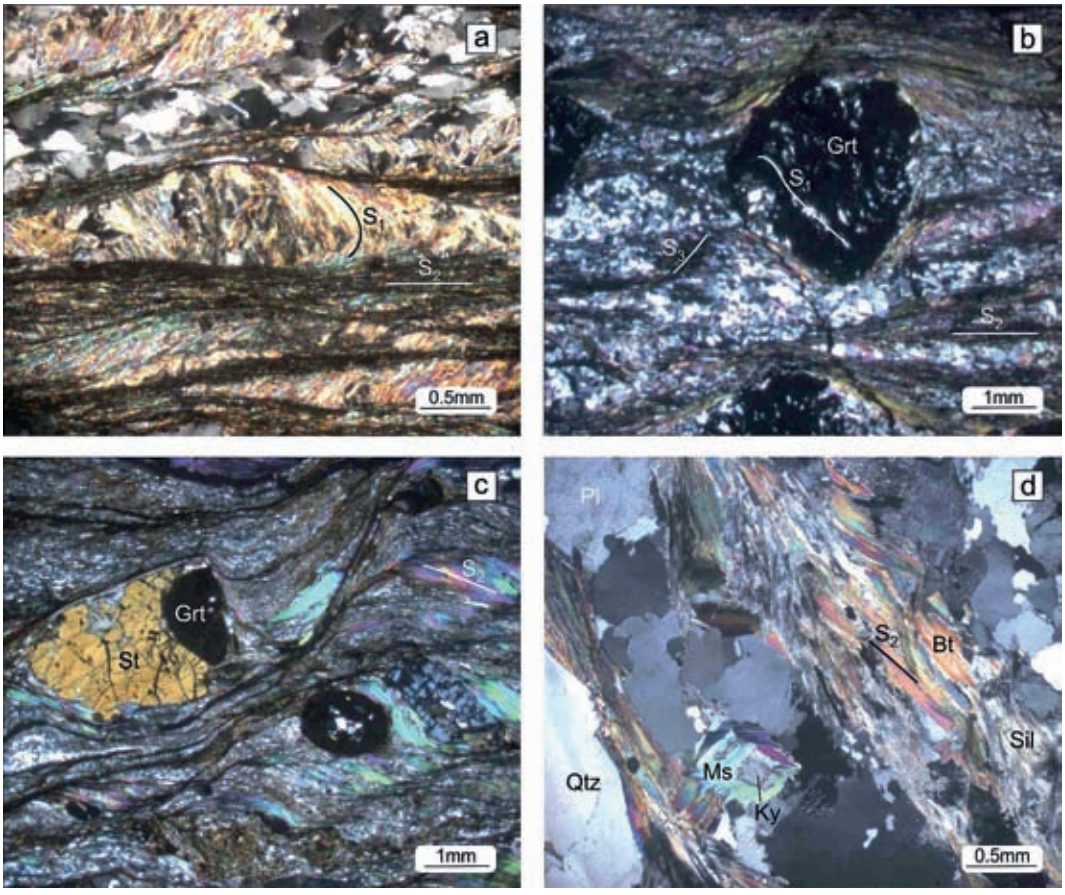

Figure 13. a) S_1 schistosity preserved in a microlithon-type microstructure in the rocks from the biotite zone; the S_2 foliation is the pervasive schistosity in the rock matrix; b) garnet porphyroblasts with quartz inclusions surrounded by S_2-oriented phyllosilicates; the inclusions in the garnet are aligned along the S_1 schistosity; c) garnet and staurolite porphyroblasts in a fine grained matrix rich in quartz and phyllosilicates; white mica occurs as mica-fish; d) kyanite surrounded by retrograde muscovite and fibrolite+biotite intergrowth in a leucosome of the Migmatite zone. All the photomicrographs are in crossed polars.

by high amounts of biotite.

The garnet (Alm: 65-72, Prp: 12-17, Grs: 3-5, Sps: 8-20 mol.%) is slightly zoned, with a general increase in spessartine content from the core to the rim, accompanied by a decrease in Fe and Mg. The matrix biotite (X_{Mg}: 0.4-0.5) contains titanium up to 0.3-0.4 a.p.f.u., while the plagioclase is an unzoned oligoclase (~ An_{20-23}) that is sometimes surrounded by a very thin rim of almost pure albite. Fibrolite is often observed in an intimate intergrowth with biotite. Muscovite is found as crystals interleaved with biotite along the S_2 foliation, as single small flakes in feldspar, and as late crosscutting crystals replacing kyanite and sillimanite (Figure 13d).

According to Cruciani et al. (2001; 2014a), the Al-silicate-bearing migmatite of NE Sardinia derived from partial melting in the kyanite stability field of a pelite/psammite sequence, followed by two stages of metamorphic re-equilibration, which included the formation of fibrolite in intergrowth with biotite, and the growth of coarse-grained muscovite.

Partial melting is thought to be syn-D_1/pre-D_2, the fibrolite formation is mainly syn-D_2, and the late formation of muscovite belongs to the post-D_2 tectonic phase.

A small lens-shaped body of amphibole-bearing migmatite was also described by Cruciani et al. (2008b; 2014b) and Massonne et al. (2013) (Figure 12b). These migmatites show discontinuous banding that is defined by alternating, well-foliated, biotite-rich mesosomes and poorly-foliated, coarse-grained quartz-feldspathic leucosomes parallel to the main foliation or folded by the D_2 tectonic phase. The leucosomes also occur as: discordant leucosomes, pods or patches up to 30-50 cm long, and pegmatite-type leucosomes. Idioblastic amphibole up to 2 cm in size can be recognized in the leucosomes, which are sometimes flanked by mafic selvedges and biotite-rich melanosomes. Tonalitic and granodioritic/granitic leucosomes were observed. The former are made up of quartz, plagioclase, ± amphibole, ± garnet (< 1-2%), minor biotite (< 5%) and trace amounts of K-feldspar. The accessory phases are apatite, zircon and titanite. Granodioritic/granitic leucosomes are only found in two lenses of amphibole-migmatite that are entrapped in the migmatized orthogneiss. They are made up of the same minerals as the tonalitic leucosomes, but with K-feldspar up to 30% of the rock volume. The mesosomes consist of the same minerals in different modal proportions (Qtz: 35-45vol.%, Pl: 35-45%, Bt: 10-20%, Am: < 5%, Grt: < 2%). Garnet (Alm: 51-53; Prp ~7; Grs: 32-34; Sps ~7 mol.%) occurs exclusively as small grains (~0.6 mm in diameter) enclosed in amphibole. Biotite growth on amphibole- and worm-like microstructures at the amphibole-biotite interface have also been observed.

Amphibole is a slightly-zoned K-rich-pargasite (X_{Mg} ~0.4-0.5), with several inclusions of plagioclase, quartz, garnet and biotite. The vast inner portion of the amphiboles has a Si content of 6.25 a.p.f.u. The outermost rims are identical in composition to the inner portion. Alternatively, in some cases, they have higher Si content up to 6.9 a.p.f.u. (Massonne et al., 2013).

The migmatized orthogneiss occurs in several localities, including, among the others, Porto Ottiolu, Tanaunella and Golfo Aranci. The Porto Ottiolu migmatized orthogneiss (Figure 12c) were studied by Palmeri (1992) and Cruciani et al. (2001). These rocks are similar to the Tanaunella orthogneiss dated at 456 ± 14 Ma by Helbing and Tiepolo (2005) and interpreted as being derived from the metamorphism of an original Ordovician calc-alkaline granitoid. The leucosomes are distinguished into folded leucosomes and leucosomes in shear zones. The former are deformed by F_2 folds with sub-vertical axes and are characterized by mafic selvedges inside the leucosome and at the boundary between the leucosome and the migmatized orthogneiss. The leucosomes emplaced along the shear zones have more faded contours and are not bordered by mafic selvedges. Some of these leucosomes are intruded along tension gashes (Corsi and Elter, 2006) in which the leucosome intrusion corresponds to a Riedel fracture system, with the master fault oriented at N 170° and R_2 at N 115°. According to Elter et al. (1999; 2010) and Padovano et al. (2012), the cm-sized shear bands with leucosome emplacement are connected to a wider extensional shear zone network in the Migmatite Complex of NE Sardinia. The mesosomes and leucosomes consist of microcline, biotite, quartz, plagioclase (An_{20-33}), ± garnet, coarse-grained retrograde muscovite

and accessory apatite, zircon and monazite. The leucosomes are granitic in composition, but the modal abundances of biotite, K-feldspar and plagioclase vary greatly between different leucosomes, but also within a given leucosome. The leucosome in the migmatized orthogneiss may be formed by the dehydratation melting of the biotite + muscovite + quartz assemblage (Palmeri, 1992). The leucosome along the shear zone may be derived from a congruent melting reaction involving the quartz-feldspatic component of the host orthogneiss, which is possibly favoured by fluid channelled along the shear zones.

Metabasites with eclogite and granulite facies relics

Metabasites with eclogite facies relics occur in northern Sardinia as bodies and lenses embedded within the L-MGMC and HGMC. These rocks have been described in some localities along the northeastern coast of Sardinia (Punta de li Tulchi, Golfo Aranci) and, further to the west, near Giuncana (north central Sardinia). Metabasites without eclogite relics appear as decametric lenses and boudins within the metapelites and quartzites of Asinara Island and Coghinas Lake, and as decametric bodies occurring along strike-slip zones within the phyllonitic belt of Posada Valley and in the HGMC.

The amphibolites from Posada Valley (Figure 10) consist of garnet, amphibole, plagioclase, Ca-pyroxene, titanite, biotite, chlorite, apatite, epidote, carbonate, albite and K-feldspar. The garnet is almandine (44-54 mol.%) and grossular-rich (29-44 mol.%), with lower amounts of pyrope (6-16 mol.%) and spessartine (0.7-6 mol.%). Despite the absence of omphacite, the amphibolites are thought to be retrogressed eclogite (Cortesogno et al., 2004).

The most investigated retrogressed eclogites of the HGMC crop out as an E-W oriented, 150 m long, 20-40 m thick lens at Punta de li Tulchi (Figures 9, 10, 12d), and are surrounded by nebulitic migmatites. According to Franceschelli et al. (1998), the Punta de li Tulchi eclogite consists of an alternation of E-W striking and 50°N dipping brownish garnet-pyroxene- rich (GP) and greenish amphibole-plagioclase-rich (AP) layers. The GP layers in turn exhibit an internal layering that is defined by alternating dark, garnet-rich, and white, clinopyroxene + plagioclase symplectite-rich, layers parallel to S_2. The adjacent AP layers consist of N 80°-SE 30° oriented millimetric white pods of plagioclase + amphibole parallel to the S_3 foliation. The S_1 schistosity is completely obliterated, and the rock foliation is defined by the orientation of amphibole crystals. The S_3 foliation, which is identified by the elongation of the white pods, is crosscut by later shear bands. In the AP layer, the modal proportion of amphibole can reach up to 50-60% of the rock volume. The metamorphic evolution of the retrogressed eclogite from Punta de li Tulchi can be summarized in the following stages: pre-symplectite, symplectite, corona and late stage (Cruciani et al., 2012). The pre-symplectite stage is documented by the occurrence of omphacite (X_{Na} up to 0.38), rutile, quartz, epidote and amphibole inclusions in garnet, and by the compositional variation of garnet from the core to the intermediate zone (core: Grs: 22-26, Prp:17-20; intermediate zone: Grs:18-23, Prp: 20-23 mol.%). The increase of pyrope and decrease of grossular content are consistent with growth during rising pressures and temperatures (prograde stage). The symplectite stage is documented by the formation of clinopyroxene+plagioclase and orthopyroxene+plagioclase symplectites (or, more rarely, orthopyroxene+plagioclase corona) around the garnet, which is the result of the breakdown of omphacite (and from the reaction between omphacite and garnet). The corona stage is characterized by the pervasive development of coronitic amphibole (magnesiohornblende to

pargasite) + plagioclase (Ab ≥ 60 mol.%) around the garnet. The pervasive growth of amphibole clearly indicates the contribution of an H_2O-rich fluid phase to the system that is more likely to be derived from an external source.

The late stage is documented by the growth of actinolite, chlorite, epidote and titanite in the rock matrix. The syn-D_4 biotite growth along the shear bands is also tentatively attributed to the late stage.

More than 50 kilometres to the north of Porto Ottiolu, the HGMC hosts a few parallel, NW-SE-oriented lenses of metabasite, with eclogite facies relics and amphibolite near to Golfo Aranci (NE Sardinia, Figure 9). All the lenses, up to a few kilometres in length, are oriented parallel to the S_2 schistosity of the surrounding migmatites. The best outcrops occur at Iles and Terrata, where two massive to poorly-foliated eclogite bodies are characterized by the alternation of garnet-rich and garnet-poor layers. In the latter, the eclogitic relics are rarely preserved and the modal amount of amphibole strongly exceeds that of the other phases, meaning that the eclogites are almost completely re-equilibrated into garnet-bearing amphibolites. Giacomini et al. (2005) distinguished the following metamorphic stages in the retrogressed eclogite of the Golfo Aranci area: prograde amphibolite, eclogite, granulite, high-temperature amphibolite and medium-temperature amphibolite. The most complete eclogitic assemblages can be found in the garnet-rich layers at the Iles locality. The mineralogical assemblage of the retrogressed eclogites includes garnet, clinopyroxene, ± orthopyroxene, amphibole, ± omphacite, ± kyanite, zoisite, plagioclase, rutile, quartz and apatite. The garnet porphyroblasts contain several inclusions of quartz, amphibole, zoisite, omphacite, rutile, apatite, kyanite, albite and zircon, which are preferentially concentrated in the garnet core. The garnet (Alm: 42-46, Prp: 23-39, Grs: 18-28, Sps: 1-4 mol.%) is compositionally zoned, with a decrease in calcium that is counterbalanced by an increase in magnesium from the core to the rim. A slightly progressive decrease in almandine and spessartine content from the core to the rim characterizes the garnet. No omphacite has ever been found in the rock matrix. Kyanite is found as inclusions in the garnet and in the rock matrix. Kyanite from the matrix is surrounded by coronitic/symplectitic microstructures consisting of an inner thin corona of anorthite (Ab: 5-10 mol.%) + spinel lamellae. This is in turn surrounded by an outer, wider and thicker corona of sapphirine lamellae + Ca-rich (Ab~20) plagioclase. Sporadically, subordinate corundum has also been found associated with these coronitic microstructures. A continuous thin layer of Na-rich plagioclase (Ab~60) frequently forms the last, outer layer of the coronitic microstructure around kyanite. Kyanite-free patchy microstructures consisting of a very fine-grained intergrowth of acicular corundum crystals + Ca-rich plagioclase (Ab~13) have also been observed. Another striking feature of the retrogressed eclogites from Iles is the occurrence of double-layered coronas of amphibole and plagioclase around garnet. These double-layered coronas consist of an inner layer of Ca-rich plagioclase (bytownite) and Al-rich amphibole (Al-pargasite, tschermakite or Mg-hornblende X_{Mg}: 0.7-0.8) surrounded by an outer layer of Ca-Na plagioclase (andesine) and amphibole.

The best example of retrogressed eclogites associated with the amphibolites hosted in the L-MGMC crop out in north-central Sardinia (Figure 7), in the Giuncana locality. The amphibolite, which mainly consists of plagioclase, amphibole, ± garnet and epidote, is derived from eclogite re-equilibration. The eclogitic bodies are embedded within micaschists and paragneisses which recorded non-coaxial deformation linked to the S_2 foliation.

The retrogressed eclogites are medium- to fine-grained, massive to poorly-schistose rocks, with

reddish millimetric garnet and green amphibole as the most abundant minerals, together with clinopyroxene, plagioclase, quartz, biotite, chlorite, epidote, ilmenite, rutile, and titanite, and accessory zircon and apatite (Cortesogno et al., 2004; Cruciani et al., 2015). The inner part of the eclogite body is poorly deformed; only the amphiboles of the outer part, close to the contact with the host micaschists, exhibit a weak shape preferred orientation consistent with the D_2 phase.

Cruciani et al. (2015) distinguished four stages in the metamorphic evolution of the Giuncana eclogites. Stage I is characterized by the occurrence of omphacite (X_{Na}: 0.4-0.5, X_{Mg}~ 0.7), epidote, quartz, amphibole, rutile and ilmenite in garnet. Omphacite has never been observed in the rock matrix. The garnet (Alm: 57-61, Prp: 10 -16, Grs: 24-30, Sps:1-3 mol.%) is chemically homogeneous or slightly zoned, with a very slight grossular decrease and a pyrope increase from the core to the rim.

Stage II is characterized by the formation of two symplectite types: amphibole (Mg-hornblende to tschermakite with X_{Mg} ~0.6) + quartz; and clinopyroxene (diopside, X_{Mg} = 0.67-0.80) + plagioclase ($X_{Na} \geq 0.80$) ± amphibole (magnesiohornblende, X_{Mg} = 0.6-0.8).

The first symplectite replaces the omphacite inclusions in the garnet, whereas the second is widespread in the matrix. Brownish biotite (X_{Mg}: 0.52-0.58) droplets and lamellae intimately growing with fine-grained oligoclase-andesine (X_{Na} = 0.63–0.79) in the matrix are also attributed to stage II.

Stage III is characterized by the widespread formation of amphibole as corona-type microstructures around the garnet and as matrix amphibole growing at the expense of symplectite. The corona type microstructures appear as a green amphibole rim or as irregular coronas of amphibole with subordinate plagioclase (X_{Na} ~0.7) around the garnet porphyroblasts. The thickness of the corona type microstructures ranges from a few tens of μm up to ~100 μm.-

The matrix amphibole replacing the symplectite often shows a pale-green core (Mg-hornblende, pargasite) that is rich in rutile needles surrounded by an Al-poorer (magnesiohornblende or actinolite) rutile-free rim. Near to the garnet crystals, the matrix amphibole develops a thin rim that is strongly enriched in Al_2O_3 (Al_2O_3 up to 14-15 wt%) (magnesiohornblende, pargasite, to Fe-pargasite, X_{Mg} = 0.44- 0.52).-

Stage IV is characterized by the local formation of biotite replacing garnet, actinolite, chlorite, albite and titanite.

Metabasites with granulite facies relics occur as a lenticular body at Montiggiu Nieddu (Figure 9). Two lithotypes have been distinguished: ultramafic amphibolites and plagioclase banded amphibolites. (Ghezzo et al., 1979; Franceschelli et al., 2002). The ultramafic amphibolite consists of igneous olivine, anorthite, clino/orthopyroxene, spinel and metamorphic minerals.

The metamorphic evolution of the Montiggiu Nieddu metabasite can be divided into three stages (Franceschelli et al., 2002):

Stage I, the granulite stage, is characterized by the development of orthopyroxene coronas, clinopyroxene, green spinel, and garnet around igneous olivine and anorthite. The garnet contains corundum inclusions. Coarse-grained orthopyroxenes include opaque mineral trails that can be interpreted as exsolution textures of an igneous Fe-rich pyroxene.

Stage II, the amphibolite stage, is represented by the pervasive growth of large amphibole grains containing coronas around olivine and plagioclase grains. Brown and green clinoamphibole, colourless amphibole and orthoamphibole replace the pyroxene and garnet. The amphibole replacing igneous pyroxene has a brown core and a green rim. The other minerals developed during the amphibolite stage are

anthophyllite, Mg-rich chlorite, plagioclase and spinel.

The minerals of stage III, the greenschist stage, mostly replace mafic minerals, and consist of tremolite, chlorite, fayalite, epidote, albite, calcite, dolomite and serpentine.

P-T conditions and P-T paths

P-T path reconstructions for a wide variety of rock types have been published for northern Sardinia by several authors (among others: Franceschelli et al., 1989 and Ricci, 1992 for the metamorphic zones of NE Sardinia; Franceschelli et al., 1998; Giacomini et al., 2005; Cruciani et al., 2012 and Cruciani et al., 2015 for eclogite-facies rocks; Franceschelli et al., 2002 for granulite-facies rocks; and Massonne et al., 2013 and Cruciani et al., 2008a; 2014a for migmatites). Although the shape and time evolution of the P-T trajectories vary in the different portions of the metamorphic basement in northern Sardinia (Franceschelli et al., 1989; 2005a; Ricci, 1992) in response to diachronous metamorphic evolution in different areas, the general P-T-t path for the Variscan metamorphism in Sardinia is clockwise, which is typical of subduction/collisional belts (England and Thompson, 1984). The P-T paths published up to now in the Variscan basement of N Sardinia are summarized in Figure 14.

Nurra region

The P-T-t path of pelitic and psammitic rocks from the Nurra region (NW Sardinia, Figures 14a, b) has been described by Franceschelli et al. (1990). In southern Nurra, a poorly constrained P-T path points to P=0.7-0.8 GPa for peak pressure at 350 °C (end of D_1) and T = 420 °C for the peak temperature at P=0.6 GPa (end of the early D_2 phase).

A metagabbro body cropping out in the chlorite zone of southern Nurra was investigated by Cruciani et al. (2011b) (P-T path 2 in Figure 14b). The P-T path of the metagabbro is a clockwise loop that is characterized by a pressure peak at ≤ 0.7 GPa and ~400 ºC. The temperature peak that occurred at ~440 ºC was accompanied by a fall in pressure to ~0.3 GPa. The final P-T evolution of the Nurra metagabbro is characterized by near-isobaric cooling to 250°-300 ºC with the formation of stilpnomelane.

In northern Nurra (P-T path 1 in Figure 14b), the end of the D_1 phase corresponds to peak pressure at 0.8 GPa at a temperature of 400 °C, while during early decompression of the D_2 phase, northern Nurra basement rocks reached peak temperatures of 450- 500 °C for pressures of 0.6-0.7 GPa. The late stage of D_2 occurred with a contemporaneous decrease in pressure (from 0.6 to 0.4 GPa) and temperature (from 480 °C to 420 °C). During the D_3 phase, the P-T decrease was: T from 420 °C to 300 °C, and P from 0.4 to 0.2 GPa.

Asinara

Limited data are available on the P-T path of the medium- and high-grade rocks of Asinara Island (NW Sardinia, Figures 14c, d), which is located only a few hundred metres north of the Nurra region. The highest P-T values calculated with conventional geothermobarometry for the D_2 phase in the L-MGMC rocks are those reported by Carosi et al. (2004a), with P= 0.8-1.0 GPa and T = 560 °C, and by Ricci (1992), with T = 600-650 °C. The first part of the P-T path shows an increase in temperature of about 100°C and a decrease in pressure of up to P = 0.2-0.3 GPa. The final part of this path shows isobaric cooling, with a temperature fall down to T = 400-500 °C. For the migmatite and high-grade rocks, Di Pisa et al. (1993) calculated a pressure fall from 0.7-0.8 GPa at 720-740 °C (migmatite stage) to 0.3-0.4 GPa at 500-600 °C (amphibolite stage). In melanosomes from the migmatites at Punta Scorno, Oggiano and Di Pisa (1998) have found kyanite relics containing sillimanite, implying the attainment of pressures

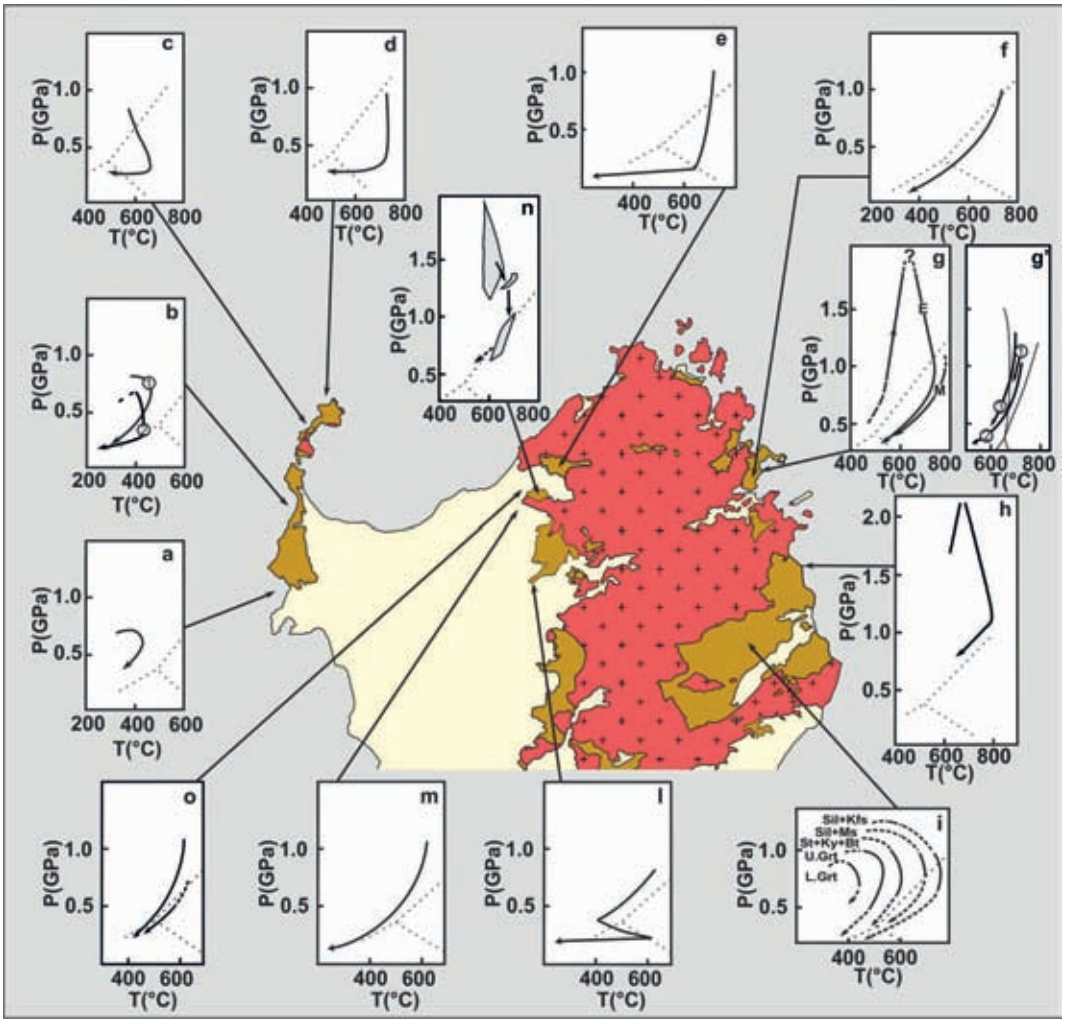

Figure 14. P-T paths from various outcrops in the northern Sardinia basement redrawn from: a,b) (Nurra) Franceschelli et al. (1990); the P-T path 2 in b is from the low-T metagabbro of central Nurra (Cruciani et al., 2011b); c,d) (Asinara Island) Carosi et al. (2004a); e,l,m) (Western Gallura, Anglona) Ricci (1992); n) Giuncana eclogite (Cruciani et al., 2015); o), L-MGMC and HGMC of the Anglona region (Carosi et al., 2009); f) (granulitic rocks from Montiggiu Nieddu) Franceschelli et al. (2002); g) (E: retrogressed eclogites and M: migmatite near Golfo Aranci) Giacomini et al. (2005); g') Punta Sirenella Al-silicate-bearing migmatites (P-T path 1, Cruciani et al., 2014a; P-T path 2, Cruciani et al., 2008a) and neighbouring amphibole-bearing migmatite (P-T path 3, Massonne et al., 2013); h) eclogitic rocks from Punta de li Tulchi from Cruciani et al. (2012); i) (metapelitic rocks from garnet to sillimanite + K-feldspar zones, NE Sardinia) Franceschelli et al. (1989), Ricci et al. (2004). U.Grt = upper garnet zone; L.Grt = lower garnet zone. Dashed line: Al_2SiO_5 triple point after Holdaway (1971).

higher than 0.8-0.9 GPa for the high-grade rocks of Asinara Island.

Anglona- Southern Gallura

The P-T-t paths for the L-MGMC and HGMC in southern Gallura (Figures 14 e,m,l,o) have a clockwise shape (Ricci, 1992; Carosi et al., 2009), and the metamorphic conditions estimated by classic thermobarometry (Carosi et al., 2009 with references) for the northern sector of the L-MGMC indicate a maximum P of 0.9-0.11 GPa and a T of 600-650 °C for the growth of syn-D_1 Barrovian mineral assemblages, and a T of 450-550 °C and a P of 0.3-0.6 GPa for syn-/late-D_2 metamorphic mineral growth.

Some differences are present in the P-T-t paths of Carosi et al. (2009) and Ricci (1992): the lack of cordierite in the HGMC and the estimated thermobaric conditions for the syn-D_2 mineral growth (0.3-0.5 GPa and 500-550 °C) constrain the HGMC path (Figure 14o) in the former's research towards a lower temperature with respect to the P-T-t path (Figure 14m) of the latter one.

Low to Medium-Grade Metamorphic Complex of NE Sardinia

For the schists and paragneisses belonging to the L-MGMC of NE Sardinia (Figure 14i), and also for the HGMC from Posada to the Punta Li Tuchi area, the P-T paths have been described by Franceschelli et al. (1989) and Ricci (1992). These authors recognized that the metamorphic peak is pre- to syn-D_2 in the garnet and staurolite zones, whereas it is syn-D_2 in the sillimanite zone. The D_1 and D_2 events are recognizable in the biotite and garnet zones, and D_1 is overprinted by D_2 in the staurolite+biotite to the sillimanite + K-feldspar zones. In this latter case, only the retrograde P-T path after the peak metamorphism is recorded by the samples, and can be reconstructed by means of conventional geothermobarometry. A brief summary of the main P-T conditions published on the Barrovian metamorphic zones of NE Sardinia are as follows: Di Vincenzo et al. (2004) calculated T = 497-544 °C, P = 1.0-1.1 GPa for the D_1 phase and T= 521-560 °C, P = 0.7-0.9 GPa for the D_2 phase in the minerals of the garnet zone using conventional geothermobarometry. For the staurolite + biotite zone, Franceschelli et al. (1989) calculated T = 610 °C, P = 0.8-1.0 GPa, while Di Vincenzo et al. (2004) estimated T = 588-624 °C, P = 0.6-0.9 GPa. As regards the kyanite + biotite zone, Carosi and Palmeri (2002) estimated T < 650 °C and P > 0.9 GPa for the D_1 phase and T = 650-700 °C, P = 0.7-0.9 GPa for D_2. For the sillimanite + K-feldspar zone (near Punta de li Tulchi), Cruciani et al. (2001) found evidence that partial melting started in the kyanite field, and then migmatite attained peak conditions in the sillimanite field at T = 700-720 °C, P= 0.6-0.8 GPa. The P-T path is consistent with thermal relaxation after a homogeneous thickening stage (Ricci, 1992).

Recently, in the chloritoid schists cropping out north of Lula village in the L-MGMC, Cruciani et al. (2013a) documented the attainment of HP conditions that preceded Barrovian-type metamorphism. The highest Si content of K-white mica and the garnet core composition suggest pressures close to 1.8 GPa and temperatures of 460-500 °C for an early stage that was characterized by the assemblage of phengitic muscovite, paragonite, chloritoid and quartz, which were frequently found as inclusions in garnet. The garnet rim composition and low Si content in K-white mica are compatible with re-equilibration at 540-570 °C and 0.7-1.0 GPa.The P-T path of the chloritoid schists matches a clockwise P-T trajectory with peak pressure before the peak metamorphism.

High-Grade Metamorphic Complex of NE Sardinia

The P-T path for the Al-silicate-bearing migmatite and amphibole-bearing migmatite north of Olbia are shown in Figure 14g,

(Cruciani et al., 2008a; 2014a; Massonne et al., 2013). The protolith of the amphibole-bearing migmatite was originally an intermediate igneous rock. Before partial melting, the H_2O stored in minerals was estimated to be nearly 1.5 wt% and the free $H_2O < 1$ wt%. At the final prograde metamorphic stage, the amphibole-bearing migmatite reached P-T conditions of about 1.3 GPa and 700 °C, at which point the melt separated from the rock to form leucosomes. Subsequently, pressure release and slight cooling resulted in the crystallization of the leucosome melt to form, among other phases, relatively large, subsequently partially resorbed, amphibole crystals. The amphibole resorption probably occurred at 0.9 GPa and 680 °C (Massonne et al., 2013).

The P-T conditions for the Al-silicate-bearing (kyanite, fibrolite) migmatites cropping out near Olbia (P-T path 1 in Figure 14g') were ~ 700°-740 °C, 1.1-1.3 GPa, which is indicative of partial melting. The P-T pseudosection calculated for the average composition of the trondhjemitic leucosomes, contoured for kyanite and biotite modal content, and for the X_{Mg} ratio in biotite, indicates P-T conditions of 660-730 °C, 0.75-0.90 GPa for the melt crystallization. According to Cruciani et al. (2008a; 2014a) and Massonne et al. (2013), only the retrograde part of the migmatite P-T trajectory can be reconstructed, as most of its prograde part was overprinted by peak metamorphism. The first, prograde portion of the migmatite P-T path was tentatively reconstructed by Giacomini et al. (2005) for the migmatitic paragneiss and felsic orthogneiss cropping out in the Golfo Aranci area of NE Sardinia (P-T path M in Figure 14g).

Metabasite with eclogite and granulite facies relicts

In the retrogressed eclogites at Punta de li Tulchi (NE Sardinia), conventional geothermobarometry (Franceschelli et al., 1998) and P-T pseudosection approach (Cruciani et al., 2012; method from Cruciani et al., 2008c) allowed to reconstruct the metamorphic history and the multistage P-T-t path of Figure 14h. This study revealed that a prograde pre-symplectite stage developed from P-T conditions of 660-680 °C and 1.6-1.8 GPa, to 660-700 °C at 1.7-2.1 GPa. This stage was followed by the formation of clinopyroxene + plagioclase and orthopyroxene + plagioclase symplectites/coronae at temperatures in excess of 800 °C and pressures in the range 1.0-1.3 GPa. Modelling the plagioclase + amphibole coronae around the garnet yielded decompression P-T conditions of 730-830 °C and 0.8-1.1 GPa. Franceschelli et al. (1998) defined temperatures of 300-400 °C and pressures lower than 0.2-0.3 GPa, which were attributed to the greenschist stage. Calculation of the H_2O (wt%) isomodes indicates that the granulitized eclogites were H_2O-undersaturated at peak-P conditions and during most of their subsequent heating and decompression, with the result that prograde garnet zoning was preserved despite the strong granulite facies overprint. The resulting P-T path consists of a small prograde segment followed by a clockwise P-T loop with diachronous peaks for pressure and temperature.

A similar P-T path (P-T path E in Figure 14g), but with an additional prograde amphibolite stage, was proposed for the retrogressed eclogites from Golfo Aranci (namely those from Iles/Terrata) by Giacomini et al. (2005). The occurrence of the edenite-andesine pair in kyanite suggests an early prograde amphibolite stage at T = 580-605 °C, P = 0.8-1.0 GPa. The HP, kyanite-bearing eclogite parageneses formed when the basic rocks were buried in a subduction-related environment; for this stage, the clinopyroxene-garnet thermometer indicates a temperature range of 580-690 °C, and maximum pressures of 1.6-1.7 GPa were obtained from the jadeite content in omphacite. Subsequently, the eclogites were re-equilibrated first under granulite facies (sapphirine-bearing parageneses: 700-800 °C, ~1.0 GPa) and then

under amphibolite facies P-T conditions.

Retrogressed eclogites hosted in the L-MGMC of Giuncana, north-central Sardinia, underwent four stages of mineralogical re-equilibration (Figure 14n). The P-T pseudosections give P-T conditions of 580 < T < 660 °C, 1.3 < P < 1.8 GPa for stage I. After stage I, a pressure decrease and temperature increase led to the breakdown of the omphacite, with the formation of clinopyroxene + plagioclase ± amphibole symplectite at ~1.25-1.40 GPa and 650°-710 °C (stage II). The P-T conditions of the amphibolite-facies with widespread amphibole formation around the garnet and in the matrix have been defined at 600-670 °C, P = 0.65-0.95 GPa (stage III). The P-T conditions of the latest stage IV are in the range of greenschist facies. The eclogites from Giuncana do not preserve any prograde segment of the P-T path, but, similar to the other Sardinian eclogites, do record a slight increase in temperature during exhumation.

The P-T history of the Montiggiu Nieddu mafic and ultramafic amphibolite (Figure 14f) was reconstructed by Ghezzo et al. (1979) and Franceschelli et al. (2002). The P-T evolution, defined by conventional thermobarometry, started with igneous crystallization and continued through the granulite (T = 700-750 °C, P ~0.8-1.0 GPa), amphibolite (T = 580-640 °C, P = 0.4-0.6 GPa), and greenschist facies (T ~330-400 °C, P < 0.2-0.3 GPa).

Tectono-metamorphic evolution for the north Sardinia basement

The knowledge acquired up to now of the L-MGMC allows us to reappraise the possible tectono-metamorphic scenario for the collisional stage of the metamorphic basement of northern Sardinia and for the intrusive sequence of the Corsica-Sardinia batholith (synoptic table in Figure 15 and Figure 16 modified from Carosi et al., in press):

- The two metamorphic complexes (namely HGMC, L-MGMC) underwent high-pressure metamorphism (testified by eclogite facies rocks and metapelites) related to the collision and/or the northwards-directed subduction of the continental crust, which was part of the northern Gondwana or peri-Gondwanian terranes in Early Palaeozoic times (Figures 16 a,b). The eclogites reached up to 1.7-2.1 GPa (Cruciani et al., 2012), whereas the metapelites reached up to 1.8 GPa (Cruciani et al., 2013a). The HP metamorphism, which is pre- to syn-D_1, was followed by Barrovian metamorphism with increasing T and P towards the northeast (Ricci et al., 2004).

- The stacking of metamorphic sequences and the consequent building-up of the nappe pile was partly contemporaneous with the HGMC exhumation, and was activated by NW-SE striking and top-to-the-S shear zones and faults with a major dip-slip component of movement. The shear zone and fault activation was driven by tectonic forces contemporaneous with the late D_1 deformation (Figure 16c).

- The HGMC continued to be exhumed during the dextral transpressional deformation, whereas the L-MGMC continued to be underthrust to the north. The D_2 deformation consisted of an orogen-parallel shearing developed along the dextral transpressional belt at the boundary between the HGMC and L-MGMC. There is prominent F_2 back-folding with a N-NE vergence (Carosi and Palmeri, 2002; Iacopini et al., 2008), which is mainly recognizable south of the transpressional belt (Figure 16d). Transpressional deformation developed at ~ 320-310 (Di Vincenzo et al., 2004; Carosi et al., 2012). Some of the oldest granitoids belonging to the U2 suite were emplaced during the overall transpressional regime at ~ 320-310 Ma (Figure 15) (Casini et al., 2012). During the final stages of the exhumation, after the transpressional deformation, an HT-LP metamorphism developed in some parts of northern Sardinia (e.g. Asinara Island: Carosi et al., 2004a; Anglona: Carosi et al., 2009 and

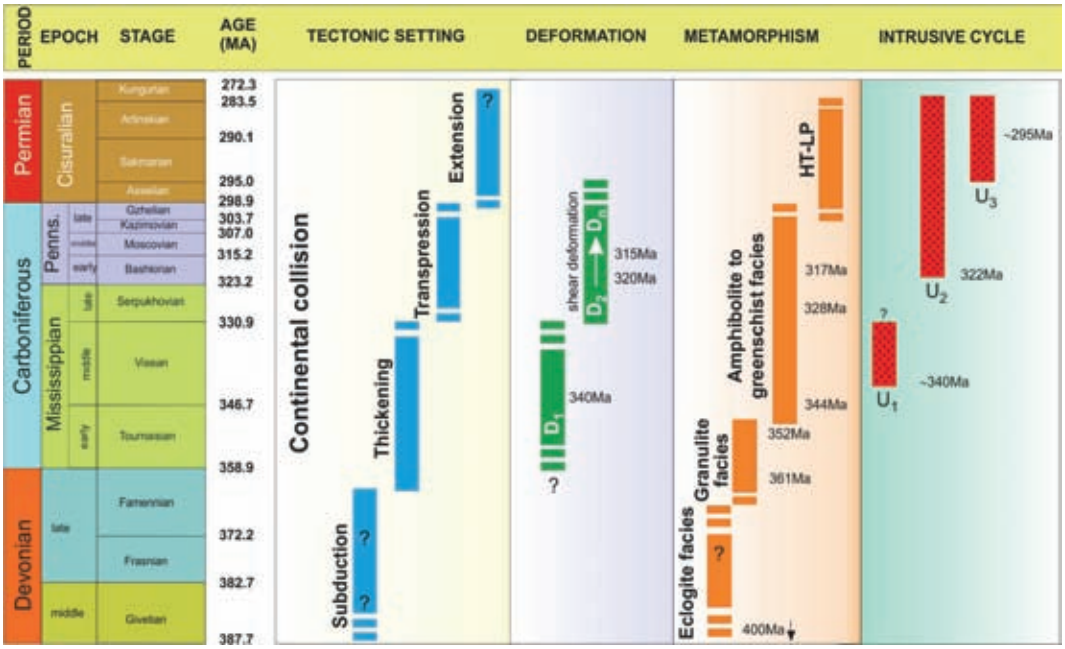

Figure 15. Synoptic table of the deformation, metamorphic and magmatic events in the Variscan basement of Sardinia. From Carosi et al. (in press).

Goceano: Casini and Oggiano, 2008). This HT-LP event could be linked to a widespread thermal anomaly induced by large granite intrusions affecting the basement at nearly 310-280 Ma. Two later deformations, again in a contractional tectonic regime, re-folded the nappe pile with orogen-parallel (NW-SE trend) and orogen-perpendicular fold axes (NE-SW trend). Later extensional tectonics affected the nappe pile at higher crustal levels with the formation of "collapse folds" and low- to high-angle normal faults.

Geodynamic framework

The Corsica-Sardinia microplate belongs to the south European branch of the Variscan Belt, for which the following evolution in Sardinia was proposed by Carmignani et al. (1992; 1994; 2001):

i) Sea-floor spreading that divided the continental margin of Gondwana from the Armorica plate, which is a process that started from the Precambrian and was active up to the Lower Cambrian.

ii) A collision between Gondwana and Armorica, with the subduction of the ocean crust below the Gondwana margin testified by the Andean-type volcanic arc products.

iii) Ocean crust subduction below the Armorica plate during the Silurian.

iv) A further continental collision between Gondwana and Armorica during the Lower Carboniferous, producing a piling up of several tectonic units.

v) Overall transpressional deformation characterized by N-S shortening and a dextral shearing, allowing the exhumation of some deep portions of the belt.

vi) A gravitative collapse of the thickened

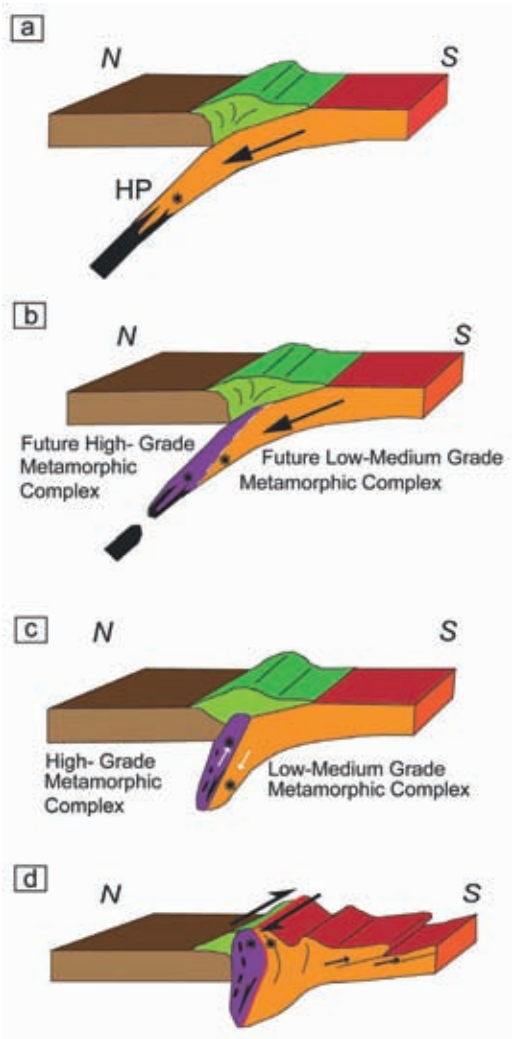

continental crust accompanied by the final ascent of some metamorphic cores.

vii) Finally, crustal extension at the upper crustal levels leading to the emplacement of calc-alkaline granitoids and contemporaneous Late Palaeozoic volcanites.

There is a consensus in the most recent literature about a strong link between Sardinia, Corsica and Maures Massif as parts of a unique Variscan microplate. As regards the relationships among the different southern European Variscan microplates, Faure et al. (2014) emphasize the analogies of the SCM microplate with the Pyrénées, Massif Central, Massif Armoricain and the Bohemian Massif. The evolution of the northern margin of Gondwana is fully discussed by Schulz et al. (2004; 2008), Giacomini et al. (2008), von Raumer and Stampfli (2008), von Raumer et al. (2013), Rossi et al. (2009), Murphy et al. (2009, 2011), Nance et al. (2011), Carosi et al., (2012), Gaggero et al. (2012), Faure et al. (2014), and Schneider et al. (2014). The available geological data led von Raumer and Stampfli (2008) and von Raumer et al. (2013) to hypothesize that a more than 10,000 km long W-E trending ribbon-like terrain comprising the future blocks of the Variscan puzzle was detached from the northern-most part of the Gondwana supercontinent. This ribbon-like piece of the continent once called the Hun Superterrane is now named the Greater

Figure 16. Proposed tectonic evolution of the Sardinian Variscides. a) collision stage at 360-340 Ma; start of the D_1 tectonic phase and HP metamorphism in the oceanic and continental crust; b) D_1 tectonic phase; HP metamorphism in the future HGMC and in the deeper part of the L-MGMC; c) late D_1 tectonic phase: thrusting of the HGMC over the L-MGMC; exhumation of the HGMC starts while the L-MGMC continues to be underthrust; d) D_2 tectonic phase during transpressional deformation between HGMC and L-MGMC. Overall exhumation with an oblique component (initial sinistral and later dextral shear sense). Orange and purple) Gondwana continental crust; purple) deeper portion of the crust undergoing HP metamorphism in the future HGMC; black) oceanic crust; green) upper crustal level of the rising Variscan Belt; brown) hinterland; asterisks) HP metamorphism. From Carosi et al. (in press).

Galatian Superterrane. In terms of the long history of the northern Gondwana margin, its breakup started 650 Ma ago, as stated by von Raumer et al. (2013) on the basis of the zircon ages obtained by Schulz et al. (2008). The next step was the emplacement 590 Ma ago of eclogitic amphibolites with an N-MORB affinity belonging to the Austroalpine basement (Schulz et al., 2004). The further evolution of the chain is characterized by the emplacement of 550-530 Ma-old volcanic arc basalts discovered in the Silvretta and Ötztal Austroalpine basement, and the following 477 Ma-aged metagabbros (Loth et al., 2001). Figure 4 in von Raumer et al. (2013) allows us to insert Sardinia in this Precambrian to Ordovician context. The figure shows the gradual opening of the Rheic ocean from west to east, i.e. from south Armorica to Central Iberia, to Cantabrian zone to Pyrenees to Montagne Noire to Maures, finally to Sardinia. The protolith ages of the Sardinian metabasites, ranging in age from 460 ± 5 to 453 ± 14 Ma, are comparable to the 450 Ma age yielded by a gabbro and to a 459 ± 4 Ma age of eclogites, both from the Argentera Massif (Rubatto et al., 2001). Further protolith ages similar to those of Sardinia are the 456.7-462 Ma obtained for the back-arc volcanites of the Penninic Métailler by Gauthiez et al. (2011). According to Schulz et al. (2004) and von Raumer and Stampfli (2008), the southern Variscan basement, including the Corsica-Sardinia microplate, underwent the following evolution. Near to the end of the Neoproterozoic, the 590 Ma-old N-MORB amphibolitic eclogites were witness to the oceanic crust of the Proto-Tethys Ocean, which was subducted southwards below the northern margin of Gondwana and represented by the Austroalpine and Helvetic domains, which are part of the Cadomia plate. The subduction produced 550-530 Ma-old calc-alkali igneous rocks. Afterwards (500-490 Ma), the opening of a back-arc basin, named as the Crypto-Rheic Ocean, took place (Schulz et al., 2004; von Raumer and Stampfli, 2008). This event is testified by the outcropping Chamrousse Ocean crust. The back-arc basin was closed soon afterwards, in the 490-480 Ma range (von Raumer and Stampfli, 2008), and the continuous southwards migrating subduction of the Proto-Tethys Ocean crust below the Cadomia microplate led to the 475 Ma-aged subduction of the mid-ocean Proto-Tethys ridge below the same microplate. Schulz et al. (2004) defined two stages named “amalgamation” (480-470 Ma) and “magmatism” (470-450 Ma), which are characterized by the emplacement of huge volumes of calc-alkali volcanic arc products and Cordillera-type intrusive granitic bodies. This time sequence of events in the 480-450 Ma age fits well with the evolution of the Helvetic, (von Raumer and Stampfli, 2008; von Raumer et al., 2013), Austroalpine (Schulz et al., 2004) and Sardinian units (Gaggero et al., 2012, and references therein). The opening of the Rheic Ocean was diachronous (Murphy et al., 2009; 2011; Nance et al., 2011); started from the west with the detachment of Avalonia and Carolinia from the northern Gondwana margin some 510-480 Ma ago; and very fast (8-10 cm/year spreading rate), leading to a maximum width of 4,000 km for the Rheic Ocean between the end of the Ordovician and the beginning of the Silurian. Except for Avalonia and Carolinia, which were completely detached from Gondwana, the other South European Variscan plates were proximal to Gondwana and separated from the supercontinent only by a sequence of back-arc basins. Avalonia and Carolinia attached to Laurussia represented the northern border of the Rheic Ocean, while the Variscan plates of central-southern Europe very near to the northern Gondwana margin marked the southern border. It is interesting to note that the protolith ages of the N-MORB eclogites related to the Rheic Ocean opening show downgrading values from north to south: the oldest values are: 490 ± 8 Ma, 495 ± 8

Ma for the Erzgebirge region (von Quadt and Günther, 1999) and 550-470 Ma for the Saxo-Thuringia region (Franke et al., 1995; Kröner et al., 2000); the intermediate values are 481 Ma for Le Bessenoits Massif, France (Paquette et al., 1995), and 470 ± 6, 472 ± 2 Ma for Ariège, Pyrénées, France (Denèle et al., 2009). The lowest age values in the range 460-450 Ma are typical of the southernmost plate of Sardinia.

As regards the Corsica-Sardinia microplate, the small extension of its bordering back-arc basins suggested to Gaggero et al. (2012) that the Cambro-Ordovician rift was an "aborted rift" in Sardinia. The following evolution of the southern branch of the Variscan Belt is defined by the 440-430 Ma-aged alkaline within-plate basalts that are similar to those observed in other southern-central European Variscan plates and interpreted by several authors (Schulz et al., 2008; Gaggero et al., 2012; von Raumer et al., 2013 and references therein) as evidence of the incipient rifting of the Palaeo-Tethys Ocean. The crustal extension revealed by alkaline within-plate basalts has been recognized in central Iberia, the Pyrénées, Sardinia, and in the Alpine domain (Austroalpine-Silvretta, Saxothuringian and Barrandian). The complex problem of the sutures among the numerous pre-Variscan plates has long been a subject of debate in the literature. As regards the Sardinia-Corsica microplate, the Posada-Asinara Line marked by the occurrence of MORB eclogites was proposed as a segment of the South Variscan suture between Armorica and the northern Gondwana margin (Cappelli et al., 1992; Carmignani et al., 1994; 2001). More recently, Rossi et al. (2009) proposed that the Armorica-Gondwana collision in Corsica was marked by the collage between the Galeria external and internal zones in a time range of 360 Ma (Tournaisian Formations) to 345-335 Ma in terms of the emplacement of Mg-K granite intrusions. According to Rossi et al. (2009), "the Eovariscan suture that delineates the collision between Gondwana and Armorica extends through Galicia, southern Brittany, southern Bohemia, the Alps, the Maures massif and the CSM (Corsica-Sardinia microcontinent), and is marked by the presence of eclogite". A more complex structural framework is proposed by Faure et al. (2014); they envisage two suture zones dividing an eastern domain from east to west (Léon-Agriates-Belgodère), a central domain of Argentella Proterozoic block = Armorica, and a western domain consisting of Solenzara-Fautea-Porto Vecchio-Zicavo-Topiti. Finally, some major tectonic lineaments that were generally considered to be suture zones are interpreted in a different way by Schneider et al. (2014); they regard the Joyeuse-Grimaud fault and the Posada-Asinara shear zone "as major vertical faults such as the La Moure Fault in the Tanneron Massif" acting "as strike-slip faults developed in the limb of large anticlines in association with Late Carboniferous intracontinental basins during the late stage of orogeny as suggested by Rolland et al. (2009) and Helbing et al. (2006)", with the suture being dismembered and folded within the Migmatite Complex of the internal zone (Schneider et al., 2014). In Sardinia also some geological elements which could originally be part of a suture, located to the North of the Corsica-Sardinia block, appears deformed and dismembered within the HGMC. However, the shearing along the Posada valley, stretching throught the northern Sardinia from west to east records a long lasting ductile history developed under a transpressional regime of deformation strictly associated to the exhumation of the Medium - to High-Grade Metamorphic Complex.

Palaeozoic sequences cropping out in Calabria-Peloritani Chain (CPC) show comparable tectonic and metamorphic history with the medium- to high-grade metamorphic rocks described in Northern Sardinia (Angì et al., 2010). However they have been deeply involved in the later Alpine collision between Eurasia and Africa (Bonardi et al., 2001 and

references therein). It is worth to note that Eo-Variscan eclogites occur also in the Sicilian strand of the CPC (Macaione et al., 2010) as part of the dismembered suture of the Southern Variscan belt.

Acknowledgements

The authors wish to thank two anonymous reviewers for helpful comments. Financial support was provided by Regione Autonoma della Sardegna, Progetti di Ricerca di base orientata, L.R. 7/2007- annualità 2010 (M. Franceschelli), and by Pisa (Resp. C. Montomoli) and Torino (Resp. R. Carosi) universities.

References

Angì G., Cirrincione R., Fazio E., Fiannacca P., Ortolano G. and Pezzino A. (2010) - Metamorphic evolution of preserved Hercynian crustal section in the Serre Massif (Cal abria-Peloritani Orogen, southern Italy). *Lithos*, 115, 237-262.

Barca S., Carmignani L., Eltrudis A. and Franceschelli M. (1995) - Origin and evolution of the Permian-Carboniferous basin of Mulargia Lake (South-Central Sardinia, Italy) related to the Late-Hercynian extensional tectonic. *Comptes Rendus de l'Académie des Sciences Paris*, 321, IIa, 171-178.

Bonardi G., Cavazza W., Perrone V. and Rossi S. (2001) - Calabria-Peloritani Terrane and northern Ionian Sea. In: Vai G.B. and Martini J.P. (Eds.), Anatomy of an orogen: the Apennines and the adjacent Mediterranean basins. Kluwer Acad., Dordrecht, 287-306.

Cappelli B., Carmignani L., Castorina F., Di Pisa A., Oggiano G. and Petrini R. (1992) - A Variscan suture zone in Sardinia: geological, geochemical evidence, Paleozoic Orogenies in Europe (special issue). *Geodinamica Acta*, 5(1-2), 101-118.

Carmignani L., Barca S., Cappelli B., Di Pisa A., Gattiglio M., Oggiano G. and Pertusati P.C. (1992) - A tentative geodynamic model for the Hercynian basement of Sardinia. In: Carmignani L., Sassi F.P. (Eds.), Contribution to the Geology of Italy with special regard to the Paleozoic basement. A volume dedicated to Tommaso Cocozza, IGCP Project N° 276, Newsletter, 5, 61-82, Siena.

Carmignani L., Carosi R., Di Pisa A., Gattiglio M., Musumeci G., Oggiano G. and Pertusati P.C., (1994) - The Hercynian Chain in Sardinia (Italy). *Geodinamica Acta*, 7, 31-47.

Carmignani L., Cocozza T., Ghezzo C., Pertusati P.C. and Ricci C.A. (1982a) - Lineamenti del basamento sardo. In: Guida alla geologia del Paleozoico sardo. Guide geologiche regionali. *Società Geologica Italiana*, 11-23.

Carmignani L., Franceschelli M., Memmi I. and Pertusati P.C. (1982b) - An example of compositional control of the celadonite content of muscovite and the incoming of biotite in the metapelites (Nurra, NW Sardinia). *Neues Jahrbuch für Mineralogie Monatsheftee*, 7, 289-311.

Carmignani L., Franceschelli M., Pertusati P.C., Memmi I. and Ricci C.A. (1979) - Evoluzione tettono-metamorfica del basamento ercinico della Nurra (Sardegna NW). *Memorie della Società Geologica Italiana*, 20, 57-84.

Carmignani L. and Oggiano G. (1997) - The variscan basement and the post-collisional evolution. Late Palaeozoic continental basins of Sardinia. The continental Permian International Congress, 15-18 Sept. 1999. Field trip guide-volume, 6-13, Pavia University.

Carmignani L., Oggiano G., Barca S., Conti P., Salvadori I., Eltrudis A., Funedda A. and Pasci S. (2001) - Geologia della Sardegna. Note illustrative della Carta Geologica della Sardegna a scala 1:200.000. Memorie della Società Geologica Italiana, 60, pp 283.

Carosi R., Cruciani G., Franceschelli M. and Montomoli C. (in press) - The Variscan Basament of Sardinia. Field guide to the excursion of the 29th Himalaya-Karakoram-Tibet Workshop, 5-8 September 2014. Società Geologica Italiana, Geological Field Trips, pp 114.

Carosi R., Di Pisa A., Iacopini D., Montomoli C. and Oggiano G. (2004a) - The structural evolution of the Asinara Island (NW Sardinia, Italy). *Geodinamica Acta*, 17(5), 309-329.

Carosi R., Di Pisa A., Iacopini D., Montomoli C., Oggiano G. and Rossi P. (2004b) - Variscan basement in north Sardinia and Corsica. Filed Trip Guide Book P11, Post Congress Field Trip, Edited by APAT, 32th International Geologic Congress, Florence, Italy, pp 20.

Carosi R., Frassi C., Iacopini D. and Montomoli C. (2005) - Post collisional transpressive tectonics

in northern Sardinia (Italy). *Journal of the Virtual Explorer*, 19, paper 3.

Carosi R., Frassi C. and Montomoli C. (2008) - Deformazione traspressiva e metamorfismo Barroviano nelle Baronie (Sardegna settentrionale). GIGS Catania, 26-29 Febbraio 2008, *Rendiconti Online della Società Geologica Italiana*, Note Brevi, 1, 68-70.

Carosi R., Frassi C. and Montomoli C. (2009) - Deformation during exhumation of medium- and high-grade metamorphic rocks in the Variscan chain in northern Sardinia (Italy). *Geological Journal*, 44, 280-305.

Carosi R., Iacopini D. and Montomoli C. (2004c) - Asymmetric folds development in the Variscan Nappe of central Sardinia (Italy). *Comptes Rendus Geoscience*, 336, 10, 939-949.

Carosi R., Montomoli C., Tiepolo M. and Frassi C. (2012) - Geochronological constraints on post-collisional shear belt in the Variscides of Sardinia, Italy. *Terra Nova*, 24 (1), 42-51.

Carosi R. and Oggiano G. (2002) - Structural evolution of Nord eastern Sardinia: insight on the tectonic evolution of the Variscan Belt. *Comptes Rendus de l'Académie des Sciences Paris*, 334, 287-294.

Carosi R. and Palmeri. R. (2002) - Orogen-parallel tectonic transport in the Variscan belt of northeastern Sardinia (Italy): implications for the exhumation of medium-pressure metamorphic rocks. *Geological Magazine*, 139(5), 497-511.

Carosi R. and Pertusati P.C. (1990) - Evoluzione strutturale delle unità tettoniche erciniche nella Sardegna centro-meridionale. *Bollettino della Società Geologica Italiana*, 109, 325-335.

Casini L., Cuccuru S., Maino M, Oggiano G. and Tiepolo M. (2012) - Emplacement of the Arzachena Pluton (Corsica-Sardinia Batholith) and the geodynamics of incoming Pangaea. *Tectonophysics*, 544-545, 31-49.

Casini L. and Oggiano G. (2008) - Late orogenic collapse and thermal doming in the northern Gondwana margin incorporated in the Variscan chain: a case study from the Ozieri Metamorphic Complex, northern Sardinia, Italy. *Gondwana Research*, 13, 396-406.

Connolly J.A.D., Memmi I., Trommsdorff V., Franceschelli M. and Ricci C.A. (1994) - Forward Modelling of Ca-silicate microinclusion and fluid evolution in a graphitic metapelites (NE Sardinia). *American Mineralogist*, 79, 960-972.

Conti P., Carmignani L. and Funedda A. (2001) - Change of nappe transport direction during Variscan Collisional evoltution of central-southern Sardinia (Italy). *Tectonophysics*, 332, 255-273.

Corsi B. and Elter F.M. (2006) - Eo-Variscan (Devonian?) melting in the High Grade Metamorphic Complex of the NE Sardinia Belt (Italy). *Geodinamica Acta*, 19 (3-4), 155-164.

Cortesogno L., Gaggero L., Oggiano G. and Paquette J.L. (2004) - Different tectono-thermal evolutionary paths in eclogitic rocks from the axial zone of the Variscan chain in Sardinia (Italy) compared with the Ligurian Alps. *Ofioliti*, 29, 125-144.

Costamagna L.G., Cruciani G., Franceschelli M. and Puxeddu M. (2012) - A volcano-sedimentary sequence with albitite layers in the Variscan basement of NE Sardinia: a petrographical and geochemical study. *Periodico di Mineralogia*, 81, 179-204.

Cruciani G., Dini A., Franceschelli M., Puxeddu M. and Utzeri D. (2010) - Metabasite from the Variscan belt in NE Sardinia, Italy: within plate OIB-like melts with very high Sr and low Nd isotope ratios. *European Journal of Mineralogy*, 22, 509-523.

Cruciani G., Fancello D., Franceschelli M., Scodina M. and Spano M.E. (2014a) - Geothermobarometry of Al-silicate-bearing migmatites from the Variscan chain of NE Sardinia, Italy: a P-T pseudosection approach. *Periodico di Mineralogia*, 83(1), 19-40.

Cruciani G., Franceschelli M., Caredda A.M. and Carcangiu G. (2001) - Anatexis in the Hercynian basement of NE Sardinia, Italy: a case study of the migmatite of Porto Ottiolu. *Mineralogy and Petrology*, 71, 195-223.

Cruciani G., Franceschelli M., Elter F.M., Puxeddu M. and Utzeri D. (2008a) - Petrogenesis of Al-silicate-bearing trondhjemitic migmatites from NE Sardinia, Italy. *Lithos*, 102, 554-574.

Cruciani G., Franceschelli M., Foley S.F. and Jacob D.E. (2014b) - Anatectic amphibole and restitic garnet in some Variscan migmatite from NE Sardinia, Italy: insights into partial melting from mineral trace elements. *European Journal of Mineralogy*, 26, 381-395.

Cruciani G., Franceschelli M. and Groppo C. (2011a) - P-T evolution of eclogite-facies metabasite from NE Sardinia, Italy: insights into the prograde evolution of Variscan eclogites. *Lithos*, 121, 135-150.

Cruciani G., Franceschelli M., Groppo C., Brogioni N. and Vaselli O. (2008c) - Formation of

clinopyroxene + spinel and amphibole + spinel symplectites in coronitic gabbros from the Sierra de San Luis (Argentina): a key to post-magmatic evolution. *Journal of Metamorphic Geology*, 26, 759-774.

Cruciani G., Franceschelli M., Groppo C., Oggiano G. and Spano M.E. (2015) - Re-equilibration history and P-T path of eclogites from Variscan Sardinia, Italy: a case study from the medium-grade metamorphic complex. *International Journal of Earth Sciences*, 104, 797-814.

Cruciani G., Franceschelli M., Groppo C. and Spano M.E. (2012) - Metamorphic evolution of non-equilibrated granulitized eclogite from Punta de li Tulchi (Variscan Sardinia) determined through texturally controlled thermodynamic modelling. *Journal of Metamorphic Geology*, 30, 667-685.

Cruciani G., Franceschelli M., Jung S., Puxeddu M. and Utzeri D. (2008b) - Amphibole-bearing migmatite from Variscan Belt of NE Sardinia, Italy: partial melting of a mid-Ordovician igneous source. *Lithos*, 102, 208-224.

Cruciani G., Franceschelli M., Marchi M. and Zucca M. (2002) - Geochemistry of metabasite from NE Sardinia, Italy: nature of protoliths, magmatic trend, and geotectonic setting. *Mineralogy and Petrology*, 74, 25-47.

Cruciani G., Franceschelli M. and Massonne H.-J. (2011b) - Low-temperature metamorphic evolution of a pre-Variscan gabbro: a case study from the Palaeozoic basement of northwest Sardinia, Italy. *Mineralogical Magazine*, 75, 2793-2812

Cruciani G., Franceschelli M., Massonne H.-J., Carosi R. and Montomoli C. (2013a) - Pressure-temperature and deformational evolution of high-pressure metapelites from Variscan NE Sardinia, Italy. *Lithos*, 175-176, 272-284.

Cruciani G., Franceschelli M., Musumeci G., Spano M.E. and Tiepolo M. (2013b) - U-Pb zircon dating and nature of metavolcanics and metarkoses from the Monte Grighini Unit: new insights on Late Ordovician magmatism in the Variscan belt in Sardinia, Italy. *International Journal of Earth Sciences*, 102, 2077-2096.

Denèle Y., Barbey P., Deloule E., Pelleter E., Olivier P. and Gleizes G. (2009) - Middle Ordovician U-Pb age of the Aston and Hospitalet orthogneissic laccoliths: their role in the Variscan evolution of the Pyrenees. *Bulletin de la Société Géologique de France*, 180(3), 209-216.

Di Pisa A., Oggiano G. (1987) - Low Pressure and High temperature metamorphic rocks in Anglona region (Northern Sardinia). *Rendiconti della Società Italiana di Mineralogia e Petrologia*, Special Issue on "Granite and their surroundings",(1987) 89-90.

Di Pisa A., Oggiano G. and Talarico F. (1993) - Post collisional tectono-metamorphic evolution in the axial zone of the hercynian belt in Sardinia: the example from the Asinara Island. *Bullettin de B.R.G.M.*, 219, 216-217, Orleans.

Di Vincenzo G., Carosi R. and Palmeri R. (2004) - The relationship between tectono-metamorphic evolution and argon isotope records in white mica: constraints from in situ ^{40}Ar-^{39}Ar laser analysis of the Variscan basement of Sardinia. *Journal of Petrology*, 45, 1013-1043.

Elter F.M., Faure M., Ghezzo C. and Corsi B. (1999) - Late Hercynian shear zones in northeastern Sardinia (Italy). *Géologie de la France*, 2, 3-16.

Elter F.M., Franceschelli M., Ghezzo C., Memmi I. and Ricci C.A. (1986) - The geology of North Sardinia. In: Guide-book to the excursion on the paleozoic basement of Sardinia. IGCP N° 5. Final Meeting Sardinia, Newletter. Special issue. 87-102.

Elter F.M., Musumeci G. and Pertusati P.C. (1990) - Late Hercynian shear zones in Sardinia. *Tectonophysics*, 176, 387- 404.

Elter F.M., Padovano M. and Kraus R.K. (2010) - The Variscan HT metamorphic rocks emplacement linked to the interaction between Gondwana and Laurussia plates: structural constraints in NE Sardinia (Italy). *Terra Nova*, 22, 369-377.

England P.C. and Thompson A.B. (1984) - Pressure temperature-time paths of regional metamorphism I. Heat transfer during the evolution of regions of thickened continental crust. *Journal of Petrology*, 25, 894-928.

Faure M., Rossi P., Gaché J., Melleton J., Frei D., Li X. and Lin W. (2014) - Variscan orogeny in Corsica: new structural and geochronological insights, and its place in the Variscan geodynamic framework. *International Journal of Earth Sciences*, 103, 1533-1551.

Ferrandini J., Gattacecca J., Ferrandini M., Deino A. and Janin M.-C. (2003) - Chronostratigraphy and paleomagnetism of Oligo-Miocene deposits of Corsica (France): geodynamic implications for the liguro-provencal basin spreading. *Bulletin de la Société Géologique de France*, 174, 357-371.

Ferrandini M., Ginsburg L., Ferrandini J., and Rossi Ph. (2000) - Présence de *Pomelomeryx boulangeri* (Artiodactyla, Mammalia) dans l'Oligocène

supérieur de la région d'Ajaccio (Corse): étude paléontologique et conséquences. *Comptes Rendus de l'Académie des Sciences Paris*, 331, 675- 681.

Fettes D. and Desmons J. (2007) - Metamorphic rocks - a classification and glossary of terms. Cambridge University Press, Cambridge, 244 pp.

Franceschelli M., Carcangiu G., Caredda A.M., Cruciani G., Memmi I. and Zucca M. (2002) - Transformation of cumulate mafic rocks to granulite and re-equilibration in amphibolite and greenschist facies in NE Sardinia, Italy. *Lithos*, 63, 1-18.

Franceschelli M., Eltrudis A., Memmi I., Palmeri R. and Carcangiu G. (1998) - Multi-stage metamorphic re-equilibration in eclogitic rocks from the Hercynian basement of NE Sardinia (Italy). *Mineralogy and Petrology*, 62, 167-193.

Franceschelli M., Mellini M., Memmi I. and Ricci C.A. (1986) - Fine-scale chlorite-muscovite association in low-grade metapelites from Nurra (NW Sardinia), and the possible misidentification of metamorphic vermiculite. *Contributions to Mineralogy and Petrology*, 93, 137-143.

Franceschelli M., Memmi I., Pannuti F. and Ricci C.A. (1989) - Diachronous metamorphic equilibria in the Hercynian basement of northern Sardinia, Italy. In: Evolution of metamorphic belts (J.S. Daly, R.A. Cliff and BW.D. Yardley eds.). *Geological Society of London, Special Publication*, 43, 371-375.

Franceschelli M., Memmi I. and Ricci C.A. (1982a) - Zoneografia metamorfica della Sardegna settentrionale. Guida alla Geologia del Paleozoico sardo, in: Guide Geologiche Regionali, Società Geologica Italiana, 137-149.

Franceschelli M., Memmi I. and Ricci C.A. (1982b) - Ca distribution between garnet and plagioclase in pelitic and psammitic schists from the metamorphic basement of north eastern Sardinia. *Contributions to Mineralogy and Petrology*, 80, 225-295.

Franceschelli M., Pannuti F. and Carcangiu G. (1991) - The formation of fibrolite nodules in a package of melanocratic gneisses from the Hercynian basement of NE Sardinia, Italy. *Schweizerische Mineralogische und Petrographische Mitteilungen*, 71, 427-439.

Franceschelli M., Pannuti F. and Puxeddu M. (1990) - Texture development and PT time path of psammitic schist from the hercynian chain of NW Sardinia (Italy). *European Journal of Mineralogy*, 2, 385-398.

Franceschelli M., Puxeddu M. and Carta M. (2000) - Mineralogy and geochemistry of Late Ordovician phosphate-bearing oolitic ironstones from NW Sardinia, Italy. *Mineralogy and Petrology*, 69, 267-293.

Franceschelli M., Puxeddu M. and Cruciani G. (2005a) - Variscan Metamorphism in Sardinia, Italy: review and discussion. *Journal of the Virtual Explorer*, 19, paper 2.

Franceschelli M., Puxeddu M., Cruciani G., Dini A. and Loi M. (2005b) - Layered amphibolite sequence in NE Sardinia, Italy: remnant of a pre-Variscan mafic silicic layered intrusion? *Contributions to Mineralogy and Petrology*, 149, 164-180.

Franceschelli M., Puxeddu M., Cruciani G. and Utzeri D. (2007) - Metabasites with eclogite facies relics from Variscides in Sardinia, Italy: a review. *International Journal of Earth Sciences*, 96, 795-815.

Franke W., Dallmeyer R.D. and Weber K. (1995) - Geodynamic evolution. In: Dallmeyer, R.D., Franke, W., Weber K. (eds) Pre-Permian Geology of Central and Eastern Europe. Springer, Berlin, 579-593.

Frassi C., Carosi R., Montomoli C. and Law R.D. (2009) - Kinematics and vorticity of flow associated with post-collisional oblique transpression in the Variscan Axial Zone of northern Sardinia (Italy). *Journal of Structural Geology*, 31, 1458-1471.

Gaggero L., Oggiano G., Funedda A. and Buzzi L. (2012) - Rifting and arc-related early Paleozoic volcanism along the north Gondwana margin: geochemical and geological evidence from Sardinia (Italy). *Journal of Geology*, 120, 273-292.

Gattacecca J. (2001) Cinématique du bassin Liguro-Provençal entre 30 et 12 Ma: Implications géodynamiques. Mémoires des sciences de la Terre, Ecole des mines de Paris, 41, 299 pp.

Gauthiez L., Bussy F., Ulianov A., Gouffon Y. and Sartori M. (2011) - Ordovician mafic magmatism in the Métailler Formation of the Mont-Fort nappe (Middle Penninic domain, western Alps)-Geodynamic implications. Abstract Volume, 9th Swiss Geoscience Meeting: Zürich, 110-111.

Ghezzo C., Memmi I. and Ricci C.A. (1979) - Un evento granulitico nella Sardegna nord-orientale. *Memorie della Società Geologica Italiana*, 20, 23-38.

Giacomini F., Bomparola R.M. and Ghezzo C. (2005) - Petrology and geochronology of metabasites with eclogite facies relics from NE Sardinia: constraints for the Palaeozoic evolution of Southern Europe.

Lithos, 82, 221-248.

Giacomini F., Dallai L., Carminati E., Tiepolo M. and Ghezzo C. (2008) - Exhumation of a Variscan orogenic complex: insights from the composite granulitic-amphibolitic metamorphic basement of South-East Corsica (France). *Journal of Metamorphic Geology*, 26, 403-436.

Helbing H., Frisch W. and Bons P.D. (2006) - South Variscan terrane accretion: Sardinian constraints on the intra-Alpine Variscides. *Journal of Structural Geology*, 28, 1277-1291.

Helbing H. and Tiepolo M. (2005) - Age determination of Ordovician magmatism in NE Sardinia and its bearing on Variscan basement evolution. *Journal of the Geological Society of London*, 162, 689-700.

Holdaway M.J. (1971) - Stability of andalusite and the aluminium silicate phase diagram. *American Journal of Science*, 271, 97-131.

Iacopini D., Carosi R., Montomoli C. and Passchier C.W. (2008) - Strain analysis and vorticity of flow in the Northern Sardinian Variscan Belt: recognition of a partitioned oblique deformation event. *Tectonophysics*, 446, 77-96.

Iacopini D., Frassi C., Carosi R. and Montomoli C. (2011) - Biases in the three-dimensional vorticity analysis using porphyroclast system: limits and application to natural examples, Special issue, 2011, *Geological Society of London, Special Publications,* 360, 301-318.

Kröner A., O'Brien J., Nemchin A.A. and Pidgeon N.T. (2000) - Zircon ages for high pressure granulites from south Bohemia, Czech Republik, and their connection to Carboniferous high temperature processes. *Contributions to Mineralogy and Petrology*, 138, 127-142.

Loth G., Elchhorn R., Holl R., Kennedy A., Schauder P. and Sollner F. (2001) - Cambro-Ordovician age of a metagabbro from the Wildschonau ophiolite complex, Greywacke Supergroup (Eastern Alps, Austria): a U-Pb SHRIMP study. *European Journal of Mineralogy*, 13, 566-577.

Macaione E., Messina A., Bonanno R. and Carabetta M.T. (2010) - An itinerary through Proterozoic to Holocene rocks in the North-Eastern Peloritani Mts. (Southern Italy). Geological Field Trips, 2(1), 98 pp.

Macera P., Ponticelli S., Del Moro A., Di Pisa A., Oggiano G. and Squadrone A. (1989) - Geochemistry and Rb/Sr of syn-tectonic peraluminous granites of Western Gallura, northern Sardinia: constraints on their genesis. *Periodico di Mineralogia,* 58, 25-43.

Massonne H-J., Cruciani G. and Franceschelli M., (2013) - Geothermobarometry on anatectic melts-a high-pressure Variscan migmatite from NE Sardinia. *International Geology Review*, 55, 1490-1505.

Miller C., Sassi F.P. and Armari G. (1976) - On the occurrence of altered eclogitic rocks in north-eastern Sardinia and their implication. *Neues Jahrbuch für Geologie und Paläontologie Monatshefte*, 11, 683-689.

Montomoli C. (2003) - Zone di taglio fragili-duttili nel basamento varisico metamorfico di basso grado della Nurra meridionale (Sardegna nord-occidentale). *Atti della Società Toscana di Scienze Naturali, Memorie*, *serie A* 108 (2002-03), 23-29.

Murphy J.B., Cousens B.L., Braid J.A., Strachan R.A., Dostal J., Kepper J.D. and Nance R.D. (2011) - Highly depeleted oceanic lithosphere in the Rheic Ocean. Implications for Paleozoic plate reconstructions. *Lithos*, 123, 165-175.

Murphy J.B., Gutierrez-Alonso G., Nance R.D., Fernandez-Suarez J., Keppie J.D., Quesada C., Dostal J. and Braid J.A. (2009) - Rheic Ocean mafic complexes: overview and synthesis. In: Murphy, J.B., Keppie, J.D. and Hynes, A.J. (eds) Ancient Orogens and Modern Analogues. *Geological Society of London, Special Publications*, 327, 343-369.

Nance R.D., Gutierrez-Alonso G., Keppie J.D., Linnemann U., Murphy J.B., Quesada C., Strachan R.A. and Woodcock N.H. (2011) - A brief history of the Rheic Ocean. *Geoscience Frontiers*, 3 (2), 125-135.

Oggiano G. (1994) - Lineamenti stratigrafico strutturali del basamento del Goceano (Sardegna centro-settentrionale). *Bollettino della Società Geologica Italiana*, 113, 105-115.

Oggiano G. and Di Pisa A. (1992) - Geologia della Catena Ercinica in Sardegna La Zona Assiale. in Struttura della Catena ercinica in Sardegna guida all'escursione. Gruppo informale di geologia strutturale 147-177, Siena.

Oggiano G. and Di Pisa A. (1998) - L'andalusite e la sillimanite nelle metamorfiti dell'Asinara: Significato geologico nel quadro dell'orogenesi ercinica. In: M. Gutierrez, A. Mattone, F. Valsecchi (Eds.) L'isola dell'Asinara: l'ambiente, la storia, il parco. Edizioni Poliedro, Nuoro, 139-144.

Oggiano G., Gaggero L., Funedda A., Buzzi L. and Tiepolo M. (2010) - Multiple early Paleozoic

volcanic events at the northern Gondwana margin: U–Pb age evidence from the Southern Variscan branch (Sardinia, Italy). *Gondwana Research*, 17, 44-58.

Padovano M., Elter F.M., Pandeli E. and Franceschelli M. (2012) - The East Variscan Shear Zone: new insights into its role in the Late Carboniferous collision in southern Europe. *International Geology Review*, 54(8), 957-970.

Palmeri R. (1992) - Petrography and geochemistry of some migmatites from northeastern Sardinia (Italy). In: L. Carmignani, F.P. Sassi (Eds). Contributions to the Geology of Italy with special regard to the Paleozoic basements. A volume dedicated to Tommaso Cocozza. IGCP No. 276, Newsletter 5: 183-186.

Paquette J.L., Monchoux P. and Couturier M. (1995) - Geochemical and isotopic study of a norite-eclogite transition in the European Variscan belt. Implications for U-Pb zircon systematics in metabasic rocks. *Geochimica et Cosmochimica Acta*, 59(8), 1611-1622.

Passchier C.W. and Trouw R.A.J. (2006) - Microtectonics. Springer Verlag, Berlin-Heidelberg-New York, 289 pp.

Ramsay J.G. (1967) - Folding and Fracturing of Rocks. McGraw-hill, New York, 568 pp.

Ricci C.A. (1972) - Geo-petrological features of the Sardinian crystalline basement. The metamorphic formations. *Mineralogica et Petrographica Acta*, 18, 235-244.

Ricci C.A. (1992) - From crustal thickening to exhumation: petrological, structural and geochronological records in the crystalline basement of northern Sardinia. In: L. Carmignani, F.P. Sassi (Eds). Contributions to the Geology of Italy with special regard to the Paleozoic basements. A volume dedicated to Tommaso Cocozza. IGCP No. 276, Newsletter 5, 187-197.

Ricci C.A., Carosi R., Di Vincenzo G., Franceschelli M. and Palmeri R. (2004) - Unravelling the tectono-metamorphic evolution of medium-pressure rocks from collision to exhumation of the Variscan basement of NE Sardinia: a review. Special issue 2: A showcase of the Italian research in metamorphic petrology. *Periodico di Mineralogia*, 73, 73-83.

Rolland Y., Corsini M. and Demoux A. (2009) - Metamorphic and structural evolution of the Maures-Tanneron massif (SE Variscan chain): evidence of doming along the transpressional margin. *Bulletin de la Société Géologique de France*, 180, 217-230.

Rossi P., Oggiano G. and Cocherie A. (2009) - A restored section of the "southern Variscan realm" across the Corsica–Sardinia microcontinent. *Comptes Rendus Geoscience*, 341, 224-238.

Rubatto D., Schaltegger U., Lombardo B., Colombo F. and Compagnoni R. (2001) - Complex Paleozoic magmatic and metamorphic evolution in the Argentera Massif (Western Alps) resolved with U-Pb dating. *Schweizerische Mineralogische und Petrographische Mitteilungen*, 81, 213-228.

Schneider J., Corsini M., Reverso-Peila A. and Lardeaux J.M. (2014) - Thermal and mechanical evolution of an orogenic wedge during Variscan collision: an example in the Maures-Tanneron Massif (SE France). In: The Variscan Orogeny: Extent, Timescale and the Formation of the European Crust. (eds.): Schulmann K., Martínez Catalán J.R., Lardeaux J.M., Janoušek V. and Oggiano G. *Geological Society of London, Special Publications*, 405, 313-331.

Schulz B., Bombach K., Pawlig S. and Brätz H. (2004) - Neoproterozoic to Early-Palaeozoic magmatic evolution in the Gondwana-derived Austroalpine basement to the south of the Tauern Window (Eastern Alps). *International Journal of Earth Sciences*, 93, 824-843.

Schulz B., Steenken A. and Siegesmund S. (2008) - Geodynamic evolution of an Alpine terrane-The Austroalpine basement in the south of the Tauern Window as a part of the Adriatic Plate (eastern Alps). In: Siegesmund, S. Fügenschuh, B., Frotzheim, N. (eds) Tectonic Aspects of the Alpine-Dinaride-Carpathian System. *Geological Society of London, Special Publications*, 298, 5-44.

Séranne M. (1999) - The Gulf of Lion continental margin (NW Mediterranean) revisited by IBS: an overview. *Geological Society of London, Special Publications,* 156, 15-36.

Simpson G.D.H. (1998) - Dehydration-related deformation during regional metamorphism, NW Sardinia, Italy. *Journal of Metamorphic Geology*, 16, 457-472.

Tikoff B. and Teyssier C. (1994) - Strain modelling of displacement field partitioning in transpressional orogens. *Journal of Structural Geology*, 16, 1575-1588.

von Quadt A. and Günther D. (1999) - Evolution of Cambrian eclogitic rocks in the Erzgebirge: a conventional and LA-ICP-MS U-Pb zircon and Sm-Nd study. *Terra Nostra*, 99(1),164.

von Raumer J.F., Bussy F., Schaltegger U., Schulz B. and Stampfli G.M. (2013) - Pre-Mesozoic Alpine basements- Their place in the European Paleozoic framework. *Geological Society of America Bulletin*, 125, 89-108.

von Raumer J.F. and Stampfli G.M. (2008) - The birth of the Rheic Ocean-Early Palaeozoic subsidence patterns and subsequent tectonic plate scenarios. *Tectonophysics*, 461, 9-20.

Submitted, March 2015 - Accepted, June 2015